TEKNISK RAPPORT · TECHNICAL REPORT 316 · 1994

ISSN 0908-3871

Research note (preliminary version) on

PORE SIZE DISTRIBUTION AND SHRINKAGE OF POROUS MATERIAL

As related to Moisture Sorption

Lauge Fuglsang Nielsen

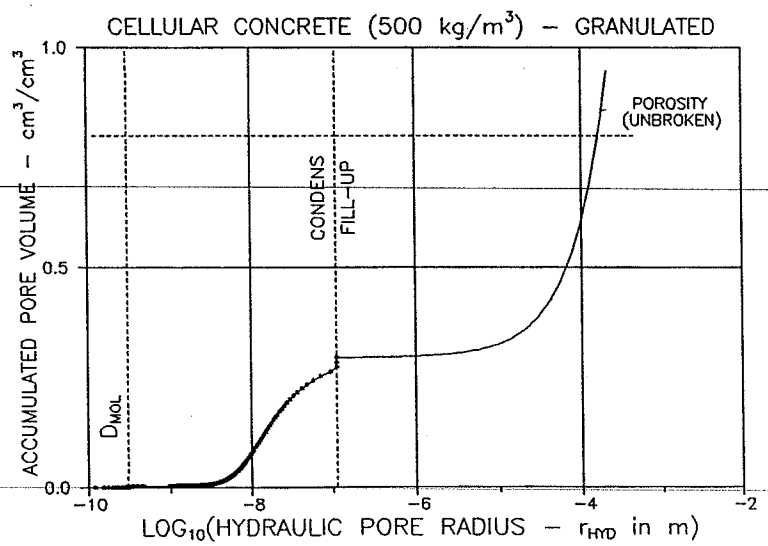

LABORATORIET FOR BYGNINGSMATERIALER
Danmarks Tekniske Højskole

BUILDING MATERIALS LABORATORY
Technical University of Denmark

Pore Size Distribution and Shrinkage of Porous Material

As related to Moisture Sorption

LAUGE FUGLSANG NIELSEN

BUILDING MATERIALS LABORATORY • TECHNICAL UNIVERSITY OF DENMARK
DK-2800 LYNGBY • DENMARK

Building Materials Laboratory
Technical University of Denmark
DK-2800 Lyngby
Telephone: 45 934331
Telefax: 45 886753

CONTENT

PREFACE

The work presented in this report is part of a major research project at the Building Materials Laboratory, Technical University of Denmark, on quantification of the pore structure in porous building materials, and the influence of pores on the mechanical and physical properties of such materials.

Moisture induced deformation of porous materials is a phenomenon of special interest in this project. A residual load is formed by a pore geometry which at the same time forms the materials stiffness. Aspects of this direct coupling between geometry, load, and response are considered in this report:

A method is developed by which pore size distributions and distributions of moisture and induced stresses in a porous material can be predicted from its (experimentally measured) capacity to attract moisture. The stress results obtained are combined with composite theory to predict deformations caused by moisture attraction (shrinkage/swelling) of the porous material considered. The practical applicability of the metods developed are demonstrated on pulp and cellular concrete materials.

The methods presented have been computerized. Software is available on special request.

ABSTRACT

Moisture is attracted by the pore system in porous materials. Attraction is associated with internal forces on the solid structure which responds by deformation according to its stiffness and geometrical complexity. The paper deals with this phenomenon such that shrinkage/swelling of porous materials can be predicted from a relatively few number of sorption experiments. Two auxiliary "tools" have been developed to obtain this result: A very efficient sorption fit method is presented by which the basic thermodynamical pore parameters (BET-parameters) can easily be deduced. A consistent pore size analysis is presented where distributions of pore volume, pore surface, and moisture content are considered simultaneously. Realiability of the methods developed are studied in a special section. Examples are given on pulp and cellular concrete in damp atmosphere.

The methods presented have been computerized. Software is available on special request.

to apply very well as a sorption description at vapour pressures less than approximately 10 %.

Unfortunately a sorption description can not be "tied up" physically at the other end of the vapour pressure scale where a relative vapour pressure of 100 % is approached. Today no relation exists between amount of capillary liquid and vapour pressure. Thus, as pressure increases we must presently accept that a description of total sorption in porous materials becomes more and more a question of mathematical fitting at higher vapour pressures. The process of fitting, however, may reveal information needed in future research on pore structures' total moisture condensing capacity. Fit parameters might be given a geometrical/physical meaning.

1.2 Steps of analysis

Three aspects of sorption in porous materials are considered. They are:

- A *generalized BET-relation* is presented by which data from total sorption tests on porous materials can be fitted very accurately. A *modified BET-relation* is included as a special plane surface version of the generalized BET-expression which considers adsorption at any vapour pressure (T-graph).

- A method is presented by which the generalized BET-description is utilized to predict *pore volume distribution, pore surface distribution* as well as distribution of moisture content in porous materials. Appropriate physical relations on moisture condensation are presented and adapted for this purpose.

- Moisture attraction is associated with internal forces on the solid structure in a porous material which responds by deformation (shrinkage or swelling) according to its stiffness and geometrical complexity. A method is presented which quantifies this phenomenon from the pore size analysis just explained such that *moisture induced deformation* of porous materials practically can be predicted directly from sorption data of the material.

- Moisture induced deformation may disturb the immidiate interpretation of a pore size analysis of soft materials. Pore expansion may produce volume enough to contain moisture not directly accounted for by the method of analysis. This phenomenon is considered in a special section at the end of the paper where the influence of materials stiffness on prediction of pore size distribution and shrinkage is discussed in more details.

1. INTRODUCTION

Information on pore size distribution is very important for any study of the mechanical and physical behavior of porous materials. Unfortunately pores are not very accessible for direct measurements. Indirect methods have to be used which involve impregnation experiments from which pressure and weight data are "translated" to pore dimensions by known physical relationships.

One important experiment of this kind is a so-called sorption test which considers the ability of a porous material to impregnate itself by liquefying an ambient gas atmosphere. The results of a sorption test are frequently presented in a sorption graph where weight at equilibrium of condensed gas (u [kg/kg solid]) is plotted against relative vapour pressure (φ).

The scopes of this paper are implicitly indicated by these introductory remarks: A method is developed by which pore size distributions and distribution of moisture induced stresses in a porous material can be predicted from its (experimentally measured) capacity to attract moisture. The stress results obtained are then combined with composite theory to predict deformations caused by moisture attraction (shrinkage/swelling) of the porous material considered. Pores considered are those accessible for molecules of the gas used in experiments.

Some general remarks and further background information on the analysis made are presented below.

1.1 Background

Two mechanisms are responsible for sorption and moisture induced deformations in porous materials: The adsorption mechanism where gas molecules liquefy on a solid surface as a result of surface force attraction - and the mechanism of capillary condensation where liquefaction is made possible by surface tension in curved vapour-liquid interfaces.

The adsorption mechanism acts at any vapour pressure. The capillary mechanism acts only as long as the tensile stress produced does not approach the strength of the liquid. Practically this means that no capillary condensation appears at low vapour pressures. (The hydraulic tensile strength of water ($\approx$ 120 MPa) is violated at a relative vapour pressure of approximately 40 %).

The phenomenon of adsorption has been studied by Brunauer, Emmett and Teller (1) who developed an expression - the so-called BET-equation - which relates amount of adsorbed liquid on a plane surface to vapour pressures less than approximately 50%. For porous materials the BET-equation is generally accepted

1.3 Systems considered - non-broken or granular

Coherent porous materials are considered with *structure defined in a dry (reference) state*. Van der Waals forces attraction between opposite faces in small pores are counterbalanced by compressive solid stresses with no harm done to the structure. The van der Waals stress-strain state of the material is considered as a "residual part" of the dry material (with influence on stiffness, strength, porosity ao.). Van der Waals forces are so strong between surfaces of distances < 2 nm that it is realistic to assume that pores cannot open up significantly by moisture intrusion. On the other hand it is also realistic to think that porous materials created in wet conditions will change (narrow) its pore structure by van der Waals forces during drying to the reference state.

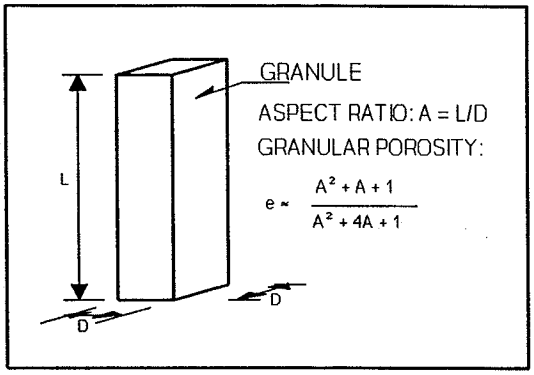

Figure 1. Aspect ratio of granule and porosity in granular system.

In the analysis systems considered are the systems exactly as they have been used experimentally to obtain sorption data. If a complete piece of the porous material considered is tested, then the results apply directly to this system. If granulation has been used to speed up sorption tests, then the results obtained refer to the granular made of the original porous material. Volume distribution, for example, refer to total pore volume of the granular which is the sum of pores in granules (of original material) and pores between granules.

Thus, unless otherwise indicated porosity c means total porosity as expressed by Equation 1,

$$c = 1 - (1 - e)(1 - c_o) \qquad (1)$$

where c_o for a moment means porosity of the original non-broken porous material. Porosity of granular system is denoted by e which can be estimated as indicated in Figure 1 which is based on information presented by the author in (2,eq.8).

Remark: Subscript "o" in Equation 1 is used only temporarily to distinguish one porosity from the other. In other sections, except Section 7.1.1, we do not use this subscript as the specific meaning of porosity is evident from the associated text.

In Section 7.1.1 c_o is temporarily introduced to deduce shrinkage of the "non-broken" (original) material from shrinkage of a granular test material.

1.4 Notations - readers guidance

A number of symbols are used in the analysis. They are summarized and briefly explained in the list of notations presented in Section 10. The terms "radius" and "vapour pressure" are used in the meaning "hydraulic radius" and "relative vapour pressure" respectively unless otherwise indicated.

Non-dimensional quantities are widely used in the analysis. As an example pore radius most often appears as radius divided by diameter of moisture molecule. Usually symbols are only explained at their first appearance in the text. Frequent consultations with the list of symbols are therefor recommended. This would also make reading easier of sections which have been written for fellow-workers mainly in the major research project previously referred (Preface Section).

The terms "shrinkage" and "swelling" are used at random. They cover similar physical phenomenons. Shrinkage is strain caused by drying. Swelling is strain caused by wetting. Whenever the terms appear the specific meaning is obvious from text and figures.

2. ADSORBED MOISTURE

2.1 Moisture content

The amount of liquid u being adsorbed on a plane surface exposed to gas at a relative vapour pressure, ϕ, is given by the BET-equation (1) reproduced in Equation 2 where u_{UNI} and C are physical constants applying to the solid/gas system considered.

$$u_{ADS} = \frac{Cu_{UNI}\phi}{(1 - \phi)(1 + [C - 1]\phi)} \qquad \textit{adsorbed moisture}$$

$$N = \frac{u_{ADS}}{u_{UNI}} = \frac{C\phi}{(1 - \phi)(1 + [C - 1]\phi)} \qquad \textit{number of molecule layers} \qquad (2)$$

The symbol u_{UNI} denotes weight of liquid when the surface is covered with a complete uni-molecular layer. The so-called BET-surface S_{BET} is related to this quantity as presented in Equation 3 where d_L is specific density of liquefied gas and D is molecule diameter. Heat properties of the system are considered by the energy factor C also presented in Equation 3 where adsorption heat of the first layer and of the next layers are denoted by W_A and W_L [J/Mol] respectively. T is absolute temperature and R is gas constant.

$$S_{BET} \approx \frac{u_{UNI}}{Dd_L} \quad with \quad Dd_L \approx 3 * 10^{-7}\ kg/m^2\ (water)$$

$$C \approx \exp\left[\frac{W_A - W_L}{RT}\right] \qquad (3)$$

Graphical representations of the BET-relation are shown in Figures 2 and 3. The following special features apply. The vapour pressure at which a complete monolyer is created is denoted by ϕ_M.

$$N = 1 \quad at\ \phi = \phi_M = \frac{1}{1 + \sqrt{C}} \quad ;\ (mono\ layer)$$

$$N \to 2 \quad at \quad \phi = \frac{1}{2} \quad when\ C \to \infty \quad ;\ (N = 1.96\ already\ at\ C = 50) \qquad (4)$$

$$N \approx \frac{\sqrt{C} - 2}{\sqrt{C}} + \frac{2(1 + \sqrt{C})}{\sqrt{C}}\phi$$
$$\phi \approx \frac{1}{1 + \sqrt{C}}\left[1 + \frac{N - 1}{2}\sqrt{C}\right] \quad \text{around} \quad \phi \approx \phi_M \tag{5}$$

Remarks: The BET-equation is, as previously indicated, developed considering a plane surface of a homogeneous solid. Forces of gravity are ignored and it is assumed that heat of condensation does not vary from the second to higher molecule layers.

It is important to recognize these assumptions when BET-parameters (C, $u_{UNI} \Rightarrow S_{BET}$) are interpreted as they are deduced from tests on porous materials. Such materials are very often composites with several components - and they have pores which are not accessible for molecules of gas used in test method. Thus, in most practice experimentally obtained BET-parameters must be considered as fit-parameters quantifying some average behaviour of the pore system considered. For example, the BET-surface obtained is a geometrical quantity which depends on how it is measured, and also to some unknown degree on materials composition.

These remarks are made only to emphasize that BET-parameters deduced from tests on porous materials should not be explained too rigorously. One should not be surprised (as shown in Section 5.3.1) that the BET-surface of wood increases with decreasing temperature. This observation does not necessarily tell that real pore surface in wood vary in this way. Future studies on the "mixture rules" of BET-parameters of porous composite materials must give the right answer to this problem. (A hypothesis on a composite C-quantity is suggested in Appendix A1 at the end of the paper which might be worthwhile testing).

2.2 Modified BET-relation - T-graph

Keeping these remarks in mind we now proceed accepting the BET-relation to be the best fit of adsorbed moisture on free surfaces at lower vapour pressures ($\phi <$ $\approx$ 40 %). At higher vapour pressures the results become increasingly bad - and quite impossible as $\phi \to 1$ where $N \to \infty$ is predicted. This feature is illustrated in Figure 2 where sorption data are shown from free surface tests on hardened cement paste (3) with energy factor $C \approx 50$.

The present analysis is therefore based on the modified BET-equation suggested in Equations 6 and 7 from which a finite number of molecule layers are predicted

for $\phi \rightarrow 1$ as shown in Figures 2 and 3. The modified BET-relation includes the original BET-relation as $\phi \rightarrow 0$. The symbols C and u_{UNI} therefor have the meanings previously explained. The modified BET-relation is the plane surface version of a more general method developed by the author in (4,5) to describe total sorption in porous materials (subsequently explained in Section 5).

The h_T function in Equation 7 is suggested by the author assuming, per hypothesis, that $N = N(\phi, N_{MAX})$ with N_{MAX} as a materials property - and that predicted results by Equation 6 should relate to the original BET-relation with trends observed from experiments such as in (3). (For future research another h_T formulation is suggested in Appendix A).

$$N = \frac{u_{ADS}}{u_{UNI}} = \frac{C\varphi h_T(\varphi)}{1 + (C - 1)\varphi} \rightarrow N_{MAX} \quad when \quad \phi \rightarrow 1 \tag{6}$$

$$h_T(\phi) = \frac{1 - \phi^{N_{MAX}}}{1 - \phi} \tag{7}$$

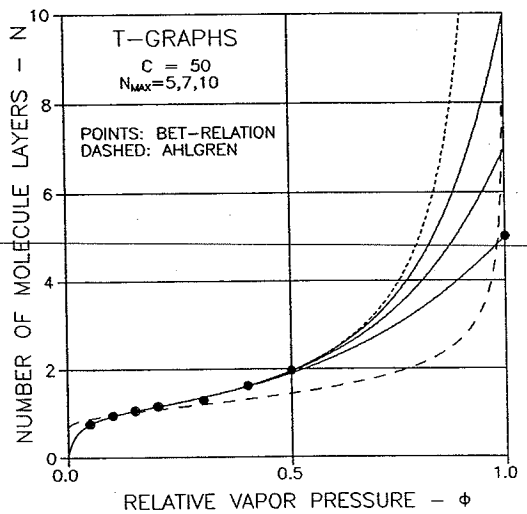

Figure 2. T-graphs for N_{MAX} = 5, 7, and 10 with C = 50. Experimental data from (3). Dashed graph is Ahlgren's expression as modified in Equation 8.

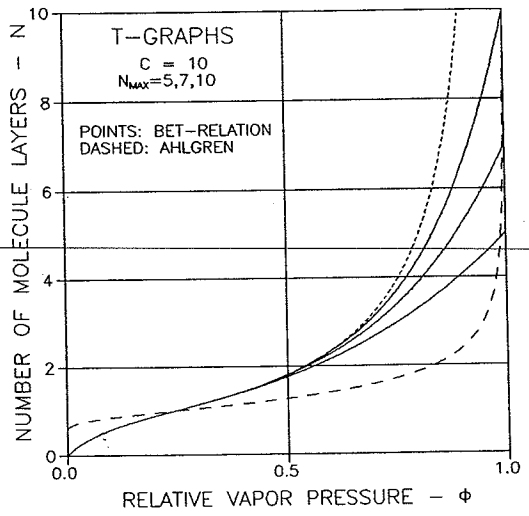

Figure 3. T-graphs for N_{MAX} = 5, 7, and 10 with C = 10. Dashed graph predicted by Equation 8.

Remark: The modified BET-relation is considered to represent the real adsorption capacity of a free surface parallel to forces of gravity. A maximum number of adsorbed molecules $N_{MAX} \approx$ 6-15 at $\phi = 1$ is generally expected in adsorption the-

ory. However, the literature only show a very limited amount of complete sorption tests on free surfaces.

Expressions, such as the modified BET-relation, which describe number of molecules or moisture thickness adsorbed on a free surface are referred to as "T-graphs" in the literature on pore size analysis. The expression presented in Equation 8 is a re-written version (monolayer vapour pressure ϕ_M introduced from Equation 4) of a T-graph suggested by Ahlgren in (6) and illustrated in Figure 2 and 3. It does not agree with the present author's expectations, considered in Equation 6, with respect to consistency between T-graphs and the basic sorption properties (C,u_{UNI}) of the specific material considered. T-graph descriptions subsequently referred to is therefor the one presented in Equation 6.

$$N = \left[\frac{\log(1/\phi_M)}{\log(1/\phi)}\right]^{1/3} = \left[\frac{\log(1+\sqrt{C})}{\log(1/\phi)}\right]^{1/3} \rightarrow \infty \text{ for } \phi \rightarrow 1$$
$$\frac{dN}{d\phi} = \frac{N}{3\phi\log(1/\phi)} \rightarrow \infty \quad \text{for both } \phi \rightarrow 0 \text{ and } \phi \rightarrow 1 \qquad (8)$$

2.3 Stresses

A number of authors have studied the stress state of adsorbed moisture. The "film pressure" and "disjoining pressure" ("micro pore pressure") results presented in this section are based on well-known principles in the field of surface chemistry as summarized in (7) for example.

2.3.1 Film pressure

An effective film pressure γ (N/m) is developed in moisture being adsorbed on a free surface. Its magnitude is given by the so-called "Gibbs-equation" developed in (8) and presented in Equation 9. An example is illustrated in Figure 5.

$$\gamma = \gamma(\phi) = \frac{RTDd_L}{M}\int_0^{\phi}\frac{N}{\phi}\,d\phi \quad \textit{film pressure in adsorbed moisture} \qquad (9)$$

2.3.2 Disjoining pressure

Two parallel surfaces with adsorbed moisture are forced together such that the distance between them is less than two times the thickness of adsorbed moisture

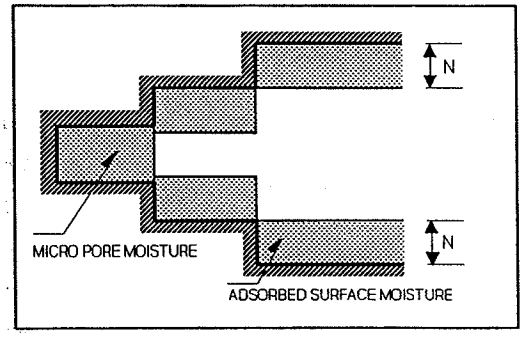

Figure 4. Model of surfaces keeping adsorbed moisture and micro pore moisture.

on a free surface. The force needed to keep the forced distance is determined by the so-called "disjoining pressure equation" developed in (9,10) and presented in Equation 10. An example of disjoining pressure prediction is shown in Figure 6.

In subsequent sections of the paper micro pores are pores filled with moisture under disjoining (hydrostatic) pressure, see Figure 4. Distance beteen opposite pore faces is too small for free surface adsorption.

Disjoining pressure between surfaces of distance $< 2N$

$$\sigma_M = \sigma_M(\phi,\phi_N) = \begin{cases} \dfrac{RTd_L}{M} \log\left[\dfrac{\phi}{\phi_N}\right] & \text{when } N(\phi) \geq 1 \text{ and } \phi \geq \phi_N \\ 0 & \text{otherwise} \end{cases} \quad (10)$$

ϕ_N *is relative vapor pressure when surface distance is just* $2N$

$$MAX(\sigma_M) = \frac{RTd_L}{M}\log\left(1 + \sqrt{C}\right) \text{ for } \phi = 1 \text{ at } \phi_N = \phi_M \text{ (mono-layer)}$$

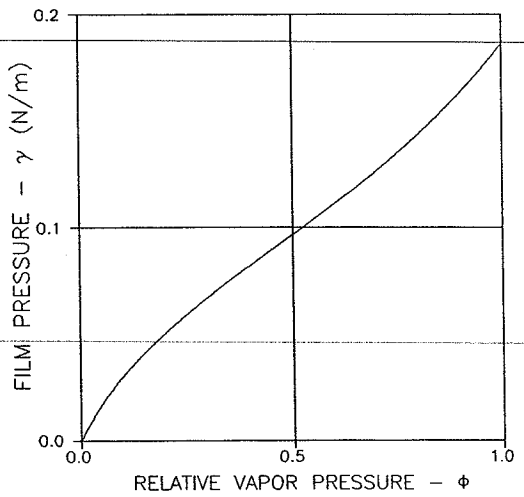

Figure 5. Film pressure in adsorbed water. N from Equation 6 with C = 10 and N_{MAX} = 6.

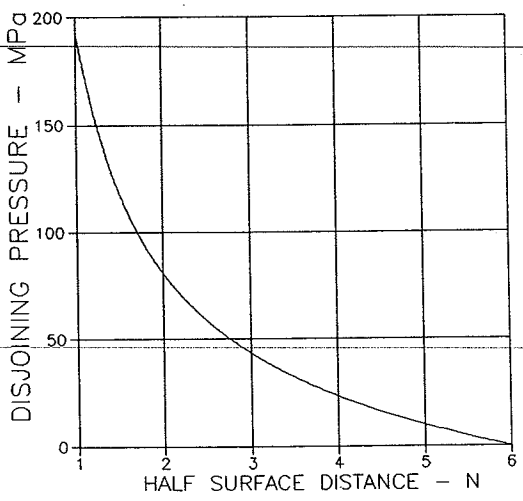

Figure 6. Disjoining pressures in adsorbed water at ϕ = 1. N from Equation 6 with C = 10 and N_{MAX} = 6.

3. CAPILLARY MOISTURE

3.1 Geometry and stress

The well-known Kelvin and Laplace relations (eg.11, Chap.6) describe meniscus radius of, and moisture stress in capillary condensed moisture. For the present purpose where pore systems are considered in general (cylindrical pores as well as slit shaped pores, a.o.) the Kelvin-Laplace relations can be written as shown in Equation 11 where θ_C and ϕ denote hydraulic radius of pore (cross-sectional area divided by respective circumference) and ambient relative vapour pressure respectively. Notice that θ_C is hydraulic radius normalized with respect to molecule diameter. A constant contact angle α (water $\alpha = 0$) between pore wall and meniscus is normally assumed. Results of Equation 11 are illustrated in Figures 7 and 8 for water at 20°C and $\alpha = 0$.

$$\theta_C = -\frac{M\,\Gamma}{RTDd_L}\,\frac{\cos\alpha}{\log\phi} \quad ; \quad \left[= \frac{\Gamma}{D\sigma_C}\right] \qquad \textit{capillary pore radius}$$

$$\sigma_C = -\frac{RTd_L}{M}\,\log\phi \quad ; \quad \left[= \frac{\Gamma\,\cos\alpha}{D\,\theta_C}\right] \qquad \textit{capillary pore tension} \qquad (11)$$

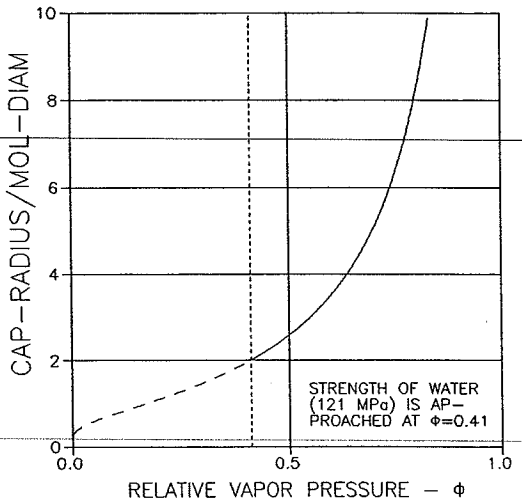

Figure 7. Meniscus radius of capillary water condensed at 20°C. $\theta_C = 362 \approx 10^{-7}$ m at $\phi = 0.995$.

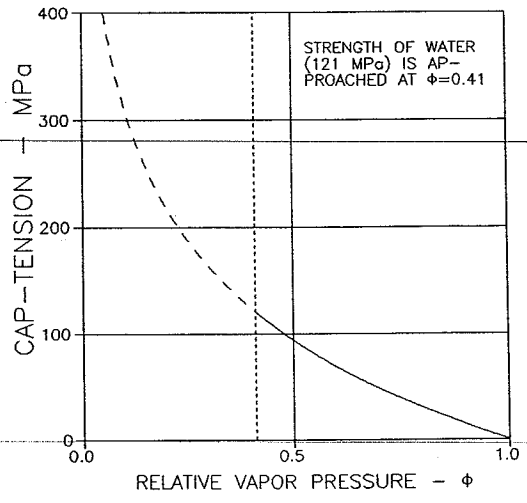

Figure 8. Tension in capillary condensed water at 20°C.

3.2 Limits of capillary condensation

Obviously capillary tension cannot exceed the moisture (hydrostatic) tensile strength which is about 110 - 120 MPa for water (12). The meniscus radius at failure is $\theta_C \approx 2$ according to Equation 11 which is the absolute lower limit of a surface defining radius. Unless otherwise informed about moisture strength we keep this observation as a failure criterion

Another limit applies to capillary condensation: Capillary forces compete with forces of gravity. In the present work it is assumed that Equation 11 cannot be applied at $\phi > 0.995$ at which pressure capillary tension becomes less than 2/3 MPa (water, 20°C, $\alpha = 0$). Moisture in porous materials at higher vapour pressures is so-called fill-up moisture considered in Section 4.

4. FILL-UP MOISTURE

At high vapour pressures (water, $\varphi > \approx 0.995$) capillary forces have to compete seriously with forces of gravity. Moisture leaks out of the pore system meaning that sorption data cannot in a reliable way be converted to geometrical quantities such as thickness or miniscus radius in Sections 2 and 3. Moisture has to be added "artificially" (so-called fill-up moisture) in order to replace lost capillary moisture and get a 100% saturation of the pore system considered. The fill-up moisture content is quantified as given by Equation 12 (4,13) where c is materials porosity. Densities of solid and liquid are denoted by d_S and d_L respectively. $u_{FOG} = u(\varphi = 1^-)$ is moisture content observed in a sorption experiment at a very high vapour pressure. A complete sorption graph is the one traditionally measured - plus a discontinuous jump of magnitude u_{FILL} at $\varphi = 1$.

$$u_{FILL} = \frac{c}{1 - c} \frac{d_L}{d_S} - u_{FOG} \qquad (12)$$

Remark: It is noticed that fill-up moisture includes moisture in pores of a granular system, see Section 1.3.

5. TOTAL SORPTION DESCRIPTION

5.1 Total moisture - generalized BET-relation

The amount of total condensed moisture in porous materials can be described by the generalized BET-relation presented in Equation 13. This relation was developed in (4,5) by the author as a rational fit expression to describe sorption in general at any vapour pressure. The original BET-relation is approached as $\varphi \rightarrow 0$ which means that the parameters C and u_{UNI} keep their meanings (as previously explained) as physical constants applying to the solid/gas system considered.

The additional parameters Q, P, and M are pore specific quantities describing the influence of pore geometry on total amount of moisture (adsorbed + capillary) attracted by a porous material. All parameters are easily determined from experimental data by the regression method suggested in Equation 14.

$$u(\varphi) = \frac{Cu_{UNI}\varphi h(\varphi)}{1 + (C - 1)\varphi} \quad ; \quad u(1) = u_{UNI}h(1)$$

with

$$h(\varphi) = \frac{1 - \varphi^{Q}}{1 - \varphi} + \frac{\varphi^{QP}}{1 - \varphi^{P}}(1 - \varphi^{PM}) \quad ; \quad h(1) = Q + M \qquad (13)$$

Remark: The comments on C and u_{UNI} obtained from experiments on porous materials apply strictly only when a complete mono-layer can be formed under free surface conditions in the pore system considered. Such conditions are implicitly assumed in this analysis. However, the remarks made in Section 2.1 should be kept in mind.

5.2 Deduction of sorption parameters

The parameters of the generalized BET-relation are determined by linearization of experimental data as shown in Equation 14. Best parameters are obtained optimizing the quality of linear regression (r^2) with respect to Q, P, and M keeping $C > 0$.

$$Y = Y_o + \alpha * X \quad \textit{linearization of Equation 13 with}$$

$$X = \varphi \quad ; \quad Y = \frac{\varphi * h(\varphi)}{u(\varphi)} \quad \textit{with fx} \quad \begin{cases} Q = 1.0, 1.5, 2.0, \ldots 5.0 \\ P = 1.0, 1.1, 1.2, \ldots 10.0 \\ M = 1.0, 1.5, 2.0, \ldots 40.0 \end{cases} \Rightarrow (14)$$

$$C = 1 + \frac{\alpha}{Y_o} \qquad u_{UNI} = \frac{1}{\alpha + Y_o}$$

General trends of the influence of the parameters are demonstrated in Figures 9 and 10: Amount of condensed moisture at lower vapour pressures (< 0.5) and at higher pressures (> 0.5) is "controlled" by Q an M respectively. Increasing amounts of moisture in these areas are described at increasing Q and M. Increasing P "flattens" moisture description at higher vapour pressures.

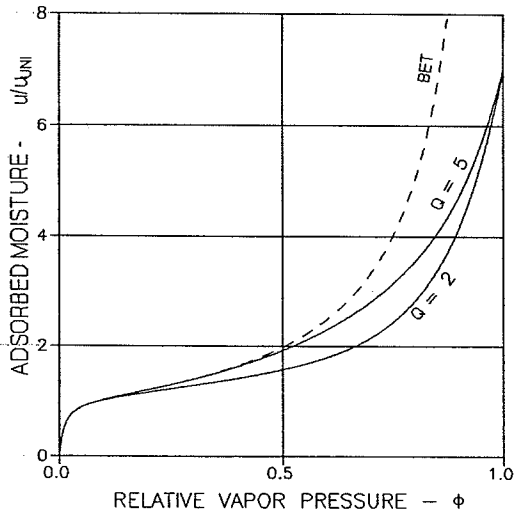

Figure 9. Sorption in porous material: Generalized BET-relation. C = 100, $(P;u_{MAX}/u_{UNI})$ = (2,7) and Q as shown.

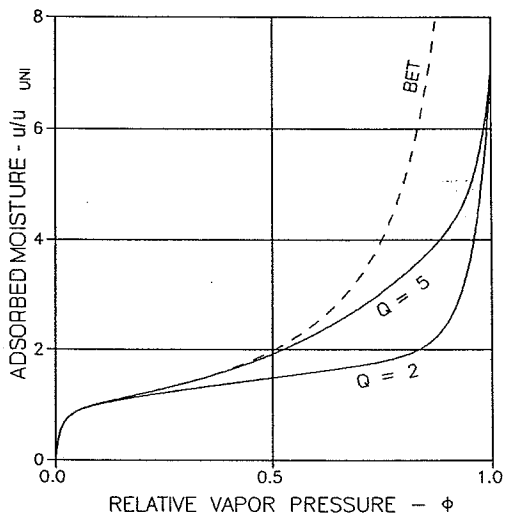

Figure 10. Sorption in porous material: Generalized BET-relation. C = 100, $(P;u_{MAX}/u_{UNI})$ = (6,7) and Q as shown.

SORP.	ADSORPTION		DESORPTION	
MATERIAL	PULP	CELL-CONCR	PULP	CELL-CONCR
Figure	11	12	11	12
Q	3.0	1.5	3.5	1.5
M	7.0	18.0	2.0	27.0
P	4.8	4.8	2.0	1.4
C	4.532	231.4	9.934	153.2
u_{UNI} [kg/kg]	0.04766	0.01802	0.05381	0.02069
FIT [r^2]	0.992	0.992	0.999	0.998
S [m^2/kg]	154231	58174	174128	66809

TABLE 1. BET-parameters and pore surfaces deduced by Equation 14.

5.3 Examples

Examples are considered in this section which illustrate the capacity of the method explained in Section 5.1 to describe moisture sorption in porous materials.

Experimental water sorption data for the examples in this section are from (14, files ENZYADS and ENZYDES) for fir-pulps produced with enzymes, and from (15,files CELCON20.501: ads and des) for crushed cellular concrete (500 kg/m^3). Sorption data are shown in Figures 11 and 12 together with descriptions obtained by Equation 13. Parameters obtained from data regression by Equation 14 are summarized in Table 1.

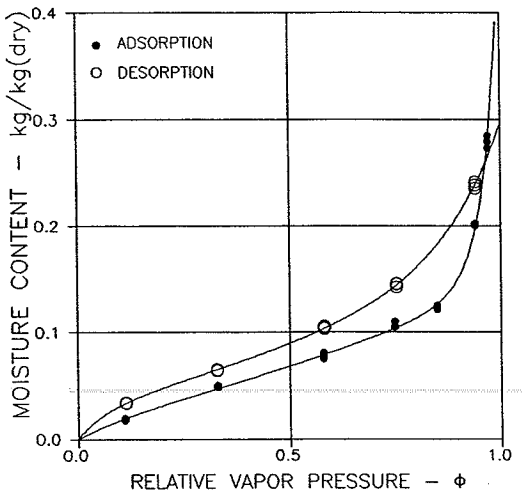

Figure 11. Pulp: Sorption isotherms.

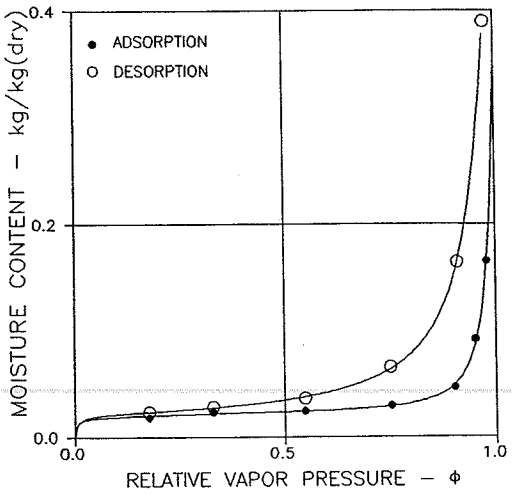

Figure 12. Cell-concrete: Sorption isotherms.

Equation 13 has also been used by the author in an analysis (4) of water sorption in wood at different temperatures. The experimental data used are from Luikov (16,17: T = -20, 20, 60, 100°C). Any regression of data was made with a fit quality better than $r^2 = 0.998$. For T > 0°C the results of the analysis can be summarized by the approximations shown in Equation 15.

It is noticed that the BET-surface of the wood considered increases with decreasing temperature. For reasons discussed in Section 2.1 this does not necessarily mean that the real pore surface varies in this way. A more plausible explanation might be that varying parts of the composite pore surface of wood are sorption active at different temperatures.

$$Q = 2 \;;\; M \approx P \approx \max(2,\ 0.040T\ [°C]) \;;\; C \approx 7.1 - 0.040T\ [°C] \qquad (15)$$
$$u_{UNI}[kg/kg] \approx 0.073 - 0.00025T[°C] \Rightarrow S[m^2/kg] \approx 243300 - 830T[°C]$$

6. PORE SIZE AND MOISTURE DISTRIBUTION

It is shown in this section how a consistent pore size analysis can be performed on a porous material for which sorption data are known from experiments. Consistency means that both pore volume and associated pore surface are described at the same pore radius - and that total porosity is described together with total pore surface at maximum pore radius.

The analysis combines the mathematical description of distributions shown in Equation 16 with a model of how a porous material impregnates itself by moisture at increasing vapour pressure respecting the information previously presented on the physics of adsorbed moisture and capillary condensed moisture. The distributions in Equation 16 are with respect to normalized pore radius θ (radius r divided by diameter D of moisture molecule).

$$G(\theta) = \frac{S}{S_{TOT}} = \int_0^{\theta} g(x)dx \quad ; \quad \textit{accumulated pore surface distribution}$$

$$H(\theta) = \frac{V}{V_{TOT}} = \int_0^{\theta} h(x)dx \quad ; \quad \textit{accumulated pore volume distribution} \qquad (16)$$

$$g(\theta) = \frac{dG}{d\theta} \qquad h(\theta) = \frac{dH}{d\theta} \quad \Big\} \quad \textit{respective density functions}$$

6.1 Model of pore filling

A pore is modelled by its surface (S) and its hydraulic radius (r) which is pore volume (V) divided by pore surface. In other words, volume of a certain pore is its surface times its hydraulic radius. This quantification of pore geometry has the advantage that more general pore shapes (ex slits or cylindres) are considered in one approach.

The state of moisture in a porous materials is modelled as follows going from vapour pressure 0 to 1:

- Adsorbed moisture is first added to the system. Adsorbed moisture is subdivided in pore filling moisture (micro pore moisture) and surface moisture on pore surface not associated with micro pores.

- Capillary condensed moisture is then added on top of the adsorbed moisture. Capillary condensed moisture is not added at relative vapour pressures greater than

a critical vapour pressure ϕ_{CR} where gravity forces dominate and capillary tension predicted by Equation 11 is less than approximately 2/3 MPa. (ϕ_{CR} = 0.995 when water is considered at 20 °C). The capillary meniscus is maintained constant for vapour pressures between $\phi = \phi_{CR}$ and $\phi = 1^-$ (state of fog). Condensation in this area is due to adsorption forces alone.

- Pore radius (r) is defined as thickness of adsorbed moisture plus hydraulic radius of capillary condensed moisture. Normalized with respect to liquid molecule diameter (D) this means, $\theta = r/D = N(\phi) + \theta_C(\phi)$ at $\phi < \phi_{CR}$ and $\theta = N(\phi) + \theta_C(\phi_{CR})$ at $\phi_{CR} \leq \phi < 1$.

The definition of pore radius as the sum of thickness of adsorbed moisture and capillary radius is quite common in pore size analysis (ex 18,19).

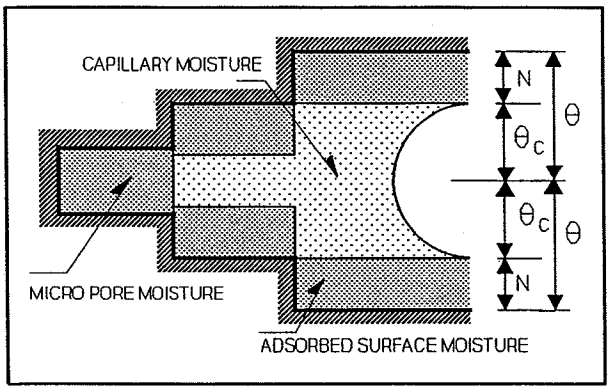

Figure 13. Definition of pore radius.

- Fill-up moisture is then added. Pores which are not filled at $\phi = 1^-$ by adsorption and capillary condensed moisture can only be filled literally by pouring plain moisture to the system. The analysis proceeds with fictitious "capillary" radii of $\theta_C = \theta - N_{MAX}$ where pore radius θ has to be known from other methods of pore size analysis - or from estimates as illustrated in Section 6.2.2

- Increase of pore volume (V) at a certain hydraulic pore radius (r) is hydraulic pore radius multiplied by increase in pore surface (S). (Look at the pore outlined in Figure 13. Increase length of last section with constant hydraulic radius such that surface of that pore increases by dS. Total pore surface will also increase with dS, while total pore volume grows with rdS). This surface-volume model (dV = rdS) couples the density functions in Equation 16 as follows,

$$\frac{h(\theta)}{g(\theta)} = \frac{dH}{dG} = \frac{\theta}{\theta_o} \quad \Rightarrow \quad \theta_o\, H(\theta) = \theta\, G(\theta) - \int_0^{\theta} G(x)\, dx \qquad (17)$$

where $\theta_o = V_{TOT}/S_{BET}/D$ is mean hydraulic pore radius of the total system considered. Note that g and h are always positive which means that G and H are monotonically increasing with pore radius.

6.2 Analysis

At any (relative) vapour pressure (ϕ) moisture content is considered as the sum of moisture (adsorbed and capillary) in filled pores and adsorbed moisture (thickness N) on pore surfaces not associated with filled pores, see Figure 14. This statement is expressed mathematically by the first expression in Equation 18 from which pore surface distribution (G) can be determined theoretically from normalized moisture content ($U = u/u_{UNI}$) as shown by the latter expression in Equation 18. This expression can be formulated as subsequently explained in Equations 19, 20, and 21 when moisture in micro pores, capillary pores, and fill-up pores respectively are considered.

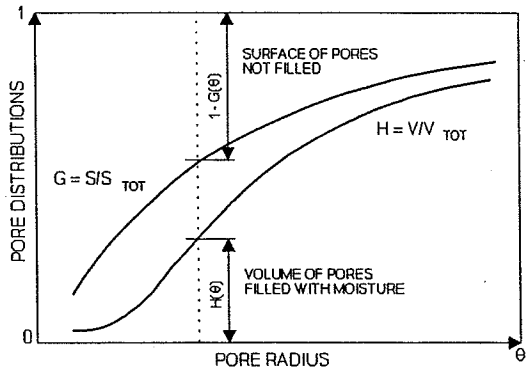

Figure 14. Contributions to moisture content of a porous material.

$$
\begin{aligned}
&u = H(\theta)V_{TOT}d_L + (1 - G(\theta))S_{TOT}N\,D\,d_L \quad \Rightarrow \\
&\qquad \textit{filled pores} + \textit{surface bound} \\
&U = \theta_o H(\theta) + N(1 - G(\theta)) \quad \Rightarrow \\
&\frac{dU}{d\theta} = \theta_o h(\theta) + [1 - G(\theta)]\frac{dN}{d\theta} - N\,g(\theta) \quad \Rightarrow \\
&\frac{dU}{d\theta} = (\theta - N)\frac{dG}{d\theta} + (1 - G(\theta))\frac{dN}{d\theta}
\end{aligned}
\qquad (18)
$$

6.2.1 Condensed moisture

Micro pores

The latter expression and the second expression in Equation 18 reduce as shown in Equation 19 when micro pores are considered with $\theta = N$. It is noticed that micro pore systems ($\theta \leq N_{MAX}$) are described by Equation 19 as long as the derivative of normalized moisture content (U) with respect to adsorbed layers (N)

is monotonically decreasing. For pore system which have nothing else than micro pores dU/dN = 0 is approached at $\phi = 1$ (indicated in subsequent Figure 20).

$$G(\theta) = 1 - \frac{dU}{dN}$$
$$H(\theta) = \frac{U - N(1 - G)}{\theta_o}$$

Micro pores (19)

Capillary pores

When pore radius becomes greater than adsorbed moisture thickness we cannot use Equation 19. Capillary moisture is added and the general expressions in Equation 18 must be used. A little re-writing gives the expressions presented in Equation 20. Notice that volume distribution is expressed just as in Equation 19.

$$\frac{dG}{d\theta} = \frac{dU/d\theta - [1 - G(\theta)]\, dN/d\theta}{\theta - N}$$
$$H(\theta) = \frac{U - N(1 - G)}{\theta_o}$$

Capillary pores (20)

6.2.2 Fill-up moisture

It is obvious from Section 6.1 that pore size analysis based on sorption data can only be made in details for radii less than $\theta = N_{MAX} + \theta_C(\phi_{CR})$ ($\approx 10^{-7}$ m). Pores with greater radii are those which can only be saturated with fill-up moisture at $\phi \equiv 1$. Pore size distributions in the fill-up area are described by Equation 21 which comes from Equation 18 (with $N \equiv N_{MAX}$) and Equation 17.

$$\frac{dG}{d\theta} = \frac{\theta_o}{\theta}\frac{dH}{d\theta} = \frac{1}{\theta - N_{MAX}}\frac{dU}{d\theta}$$
$$H = \frac{U - N_{MAX}(1 - G)}{\theta_o}$$

Fill-up pores (21)

As we do not know pore sizes in the fill-up area we may proceed introducing some estimates on pore surface, pore volume or moisture content. The following analytically closed form solutions are the results of using Equation 21 with a log-

linear variation of pore surface distribution. Other solutions are presented in Appendix A.

Log-linear pore surface distribution

$$G = G_{MIN} + (1 - G_{MIN})\frac{\log(\theta/\theta_{MIN})}{\log(\theta_{MAX}/\theta_{MIN})} \Rightarrow$$

$$U = U_{MIN} + \frac{1 - G_{MIN}}{\log(\theta_{MAX}/\theta_{MIN})}\left[\theta - \theta_{MIN} - N_{MAX}\log\left[\frac{\theta}{\theta_{MIN}}\right]\right] \quad (22)$$

Subscript "MIN" indicates value corresponding to $\phi = 1^-$

Volume distribution is derived from Equation 21. At maximum filling of pore system ($G = G_{MAX} = 1$) we get the following expression from which maximum pore radius can be determined.

$$\theta_{MAX} = \theta_{MIN} + \left[\frac{U_{FILL}}{1 - G_{MIN}} + N_{MAX}\right]\log\left[\frac{\theta_{MAX}}{\theta_{MIN}}\right] \quad (23)$$

6.2.3 Moisture distribution

The contents of micro pore moisture, surface moisture, and capillary moisture are related to pore size distributions as given in Equation 24. This is a consequence of the considerations made in Section 6.2 (Equation 18 and Figure 14).

$$\begin{aligned}
U_M &= \theta_o * H(N) && \textit{micro pore moisture}\\
U_S &= N[1 - G(N)] && \textit{surface moisture, adsorbed outside micro pores}\\
U_A &= U_M + U_S && \textit{adsorbed moisture in total}\\
U_C &= U - U_A && \textit{capillary moisture}\\
U_{FILL} &= U_{TOT} - U(\phi{=}1^-) && \textit{fill-up moisture at } \phi = 1
\end{aligned} \quad (24)$$

6.2.4 Procedure of analysis

The analysis proceeds as follows:

- Calculation runs stepwise with vapour pressure as independent variable starting with $\phi = 0$. Useful information on closed form analytical differentation of modified and generalized BET-relations are presented in (13).

- Estimate $N_{MAX} \approx 10$. Look at the results. Vary N_{MAX} according to the following conditions:
- First appearance of cappilary moisture must exceed $\phi \approx 0.4$.
- Distribution G (and H) must increase monotonically towards a value of 1 at the same pore radius r_{MAX}.
- Calculation stops when these criteria are satisfied.

6.3 Examples

Some examples of pore size analysis are demonstrated in this section. Notice that the results refer to total system including surfaces and volumes made by granulation - unless otherwise indicated.

MATERIAL	PULP	CELL-CONCR
Figures	Section 6.3.1	Section 6.3.2
d_S [kg/m^3]	1500	2650
c	0.5	0.8
A, e	100, 0.97	1, 0.5
r_{MAX} [m]	$\approx 10^{-5}$	$\approx 10^{-3}$

TABLE 2. Material parameters. Same materials as in Table 1. r_{MAX} is estimated representative maximum hydraulic pore radius.

Water desorption data are used all-over. Log-lin G-distributions are assumed in fill-up areas. The mate-rials considered are the pulp and cellular concrete previously referred to in Section 5.3 and Table 1. Further material parameters are presented in Table 2.

6.3.1 Pulp

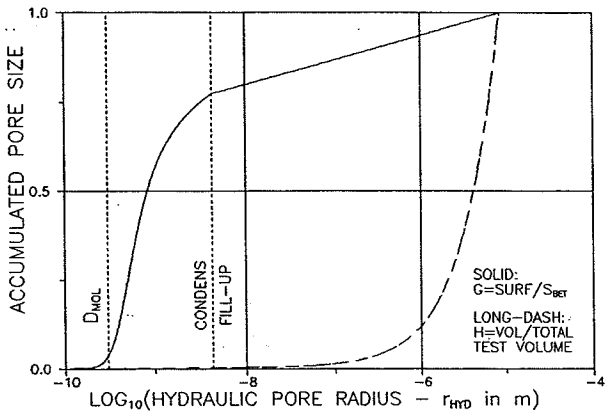

Figure 15. Pulp: Pore size distribution. *Notice* that true CONDENS-FILL-UP transition is at $r_{HYD} \approx 10^{-7.0}$ m. Thus, real distributions are constants between $r_{HYD} = 10^{-8.4}$ m and that radius. See subsequent remark at end of this section.

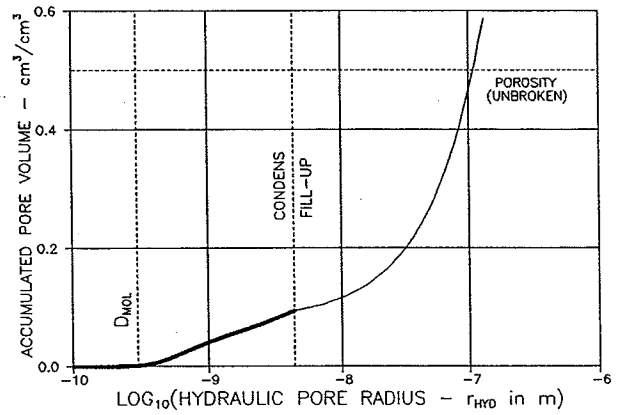

Figure 16. Pulp: Accumulated pore volume (relative to volume of un-broken material).

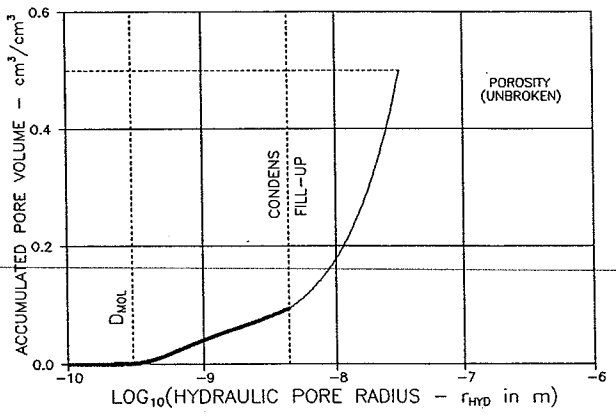

Figure 17. Pulp: Accumulated pore volume if non-broken test specimens (e = 0) are assumed. Notice that $r_{MAX} \approx 10^{-5}$ m is not maintained under this assumption.

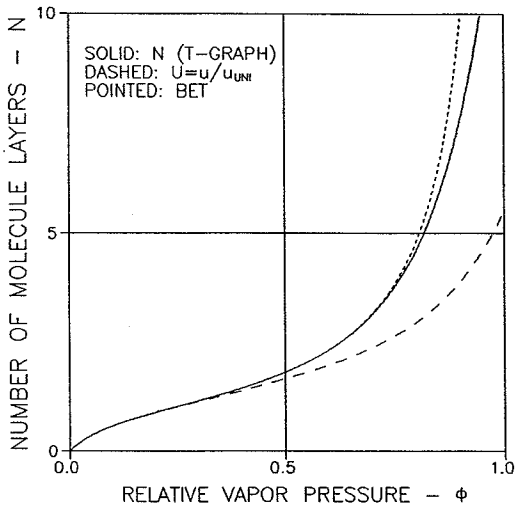

Figure 18. Pulp: T-graph (N_{MAX} = 14) and normalized moisture (U).

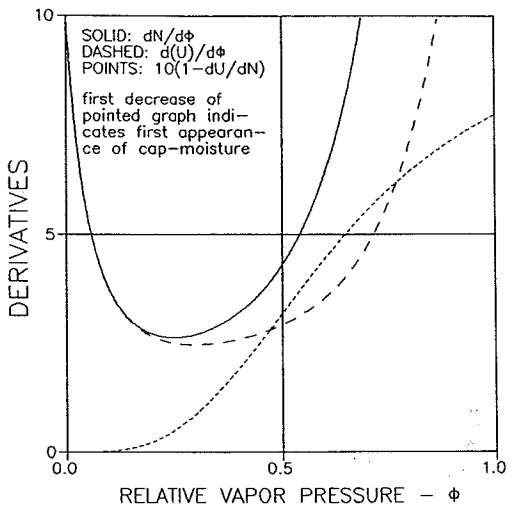

Figure 19. Pulp: Derivatives of T-graph and normalized moisture content.

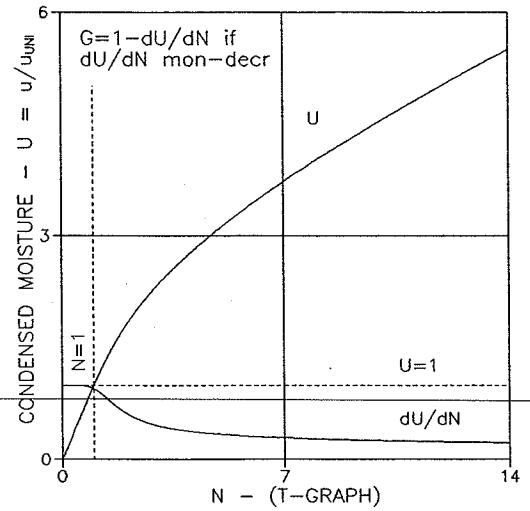

Figure 20. Pulp: U-N-graph and dU/dN. Notice, initial slope dU/dN = 1.

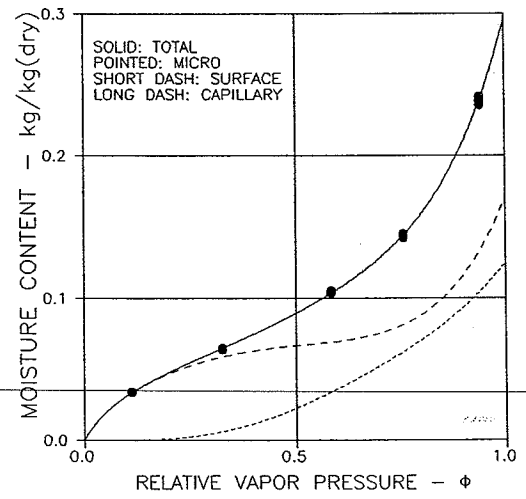

Figure 21. Pulp: Moisture distribution.

Remark: Obviously there is no capillary space in pulp which can be detected from water desorption data. Fill-up moisture starts at radii of magnitudes $> \approx 10^{-7}$ m (see Figure 7). This means (see Figure 15) that pulp has a lack of pores of radii between $10^{-8.5}$ m and at least 10^{-7} m which can only be detected by other means than by sorption data. We recall from Section 6.2.2 that the theoretical fill-up results shown in the figures are due to estimates introduced exactly because of lacking information from other methods.

6.3.2 Cellular concrete

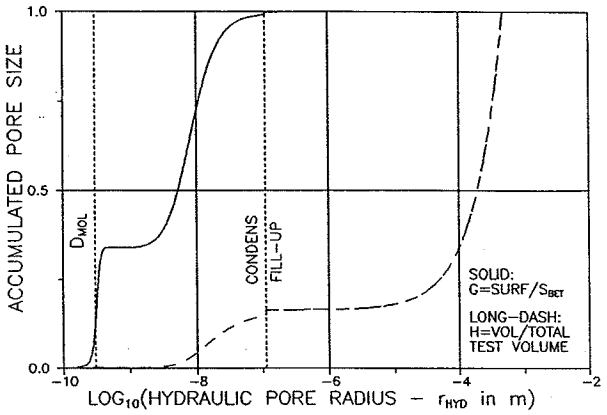

Figure 22. Cell-concrete: Pore size distribution.

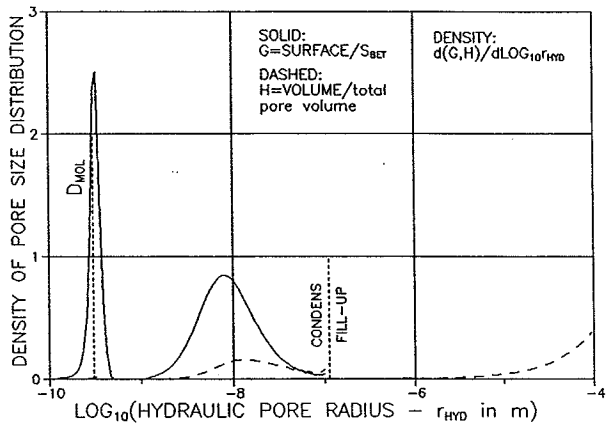

Figure 23. Cell-concrete: Density of pore size distribution.

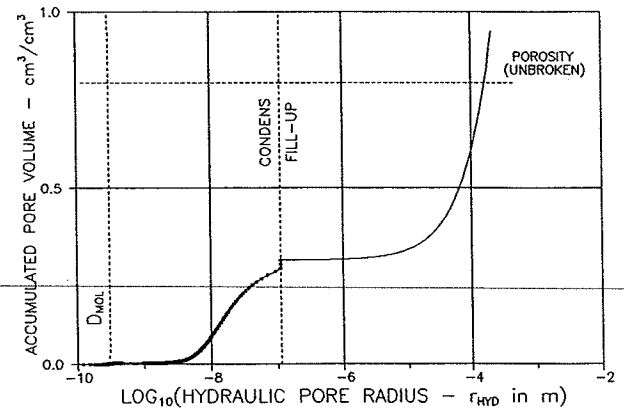

Figure 24. Cell-concrete: Accumulated pore volume (relative to volume of un-broken material).

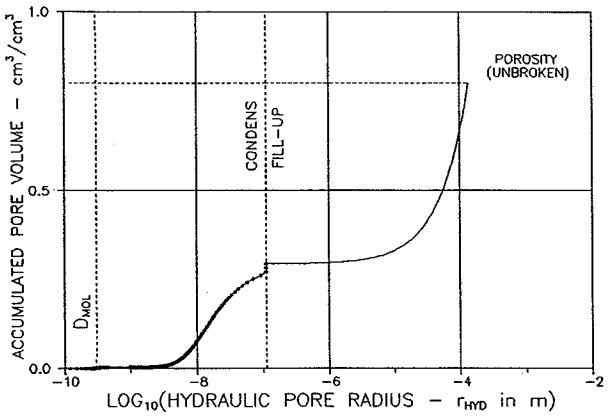

Figure 25. Cell-concrete: Accumulated pore volume if non-broken test specimens (e = 0) are assumed. Notice that $r_{MAX} \approx 10^{-3}$ m is not maintained under this assumption.

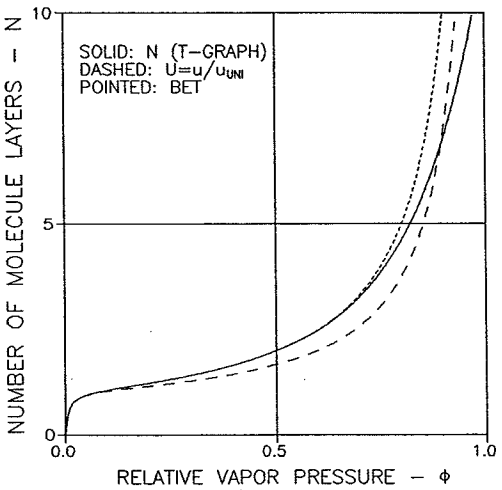

Figure 26. Cell-concrete: T-graph (N_{MAX} = 11.5) and normal. moist. content (U).

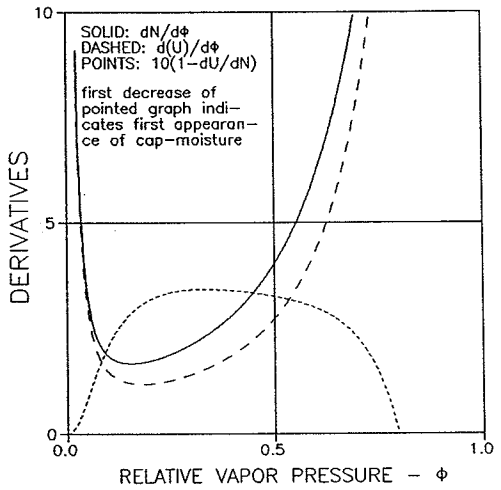

Figure 27. Cell-concrete: Derivatives of T-graph and normalized moisture.

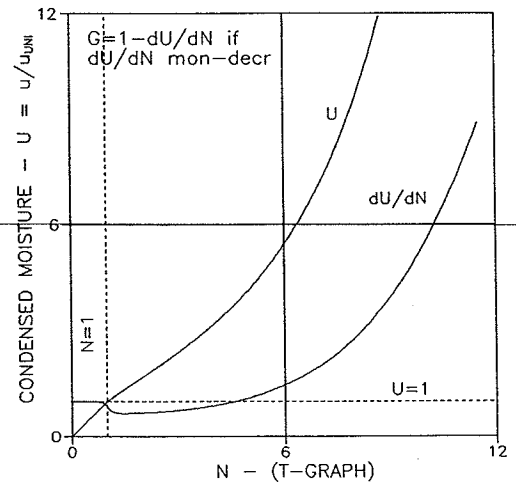

Figure 28. Cell-concrete: U-N-graph and dU/dN. Notice, initial slope is 1.

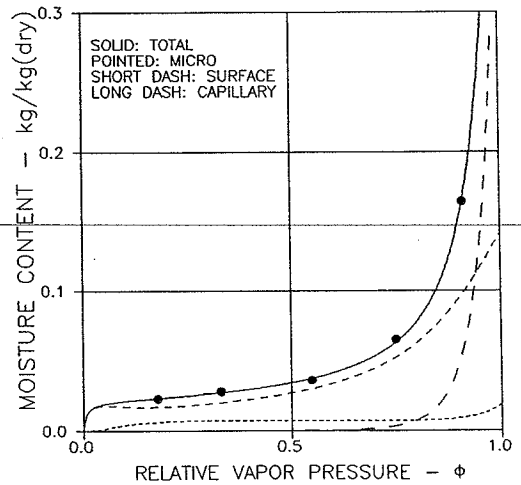

Figure 29. Cell-concrete: Moisture distribution.

7. SHRINKAGE AND SWELLING

There are two concepts of explaining moisture induced strain, shrinkage/swelling, of porous materials. Bangham et al. (20) suggested that the adsorption mechanism is the prime mechanism causing shrinkage. Powers (12), however, argued very convincingly that important cases cannot be explained without also considering the effects of micro pore pressures (disjoining pressure). The model suggested by Powers in (12) states that shrinkage of porous materials can only be explained in general by a combination of all three sorption mechanisms previously considered in this paper: Adsorption, disjoining pressure, and capillary tension. The shrinkage/swelling analysis presented in this section quantifies the ideas of Powers. The present authors porous materials stiffness theory presented in (fx 21,22) is used to predict shrinkage/swelling as strain caused by pore pressure. Pore pressure is determined from the amounts of condensed moisture detected in pore size analysis - and from the stress states of these contributions.

Remark: A simple alternative generation of the stiffness properties of porous materials is presented in Appendix B at the end of the paper.

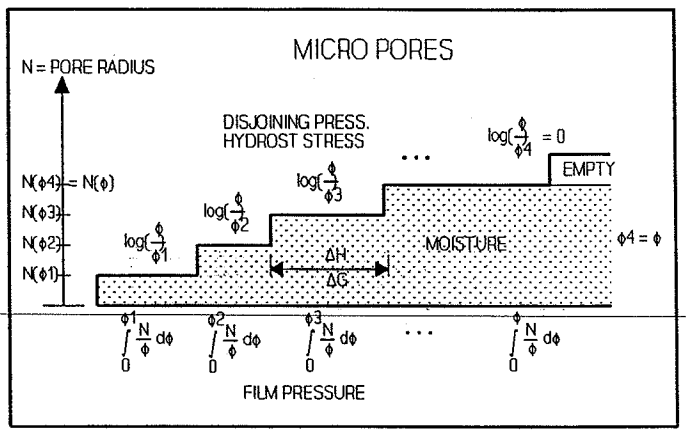

Figure 30. Micro pore stresses and surface film pressure. Constants omitted.

7.1 Pore pressure and tension

The surface average ($<\gamma>$) of adsorbed film pressure is determined by the first expression in Equation 25 from the film pressure solution presented in Equation 9 with surface weights introduced from the model shown in Figure 30 combined with the pore surface distribution analysis previously made in Section 6.

The pressure effect of the adsorbed film pressure ($<\sigma_\gamma>$) on pore walls is then calculated from the second expression in Equation 25 developed by the author from a stress analysis made by Flood (23) on particles subjected to surface

tension. It is noted that the pressure calculated acts hydrostatically on the total solid phase surface (pore surface and external surface).

The volume average of micro pore pressures from $\phi = 0$ to ϕ is calculated as shown in Equation 26 from the single micro pore solution in Equation 10 with volume weights introduced from the model shown in Figure 30 combined with the pore volume distribution analysis previously made in Section 6.

The volume average of capillary moisture tension is calculated very easily as shown in Equation 27 with σ_C from Equation 11 and moisture contents as previously determined in the analysis of pore size distribution.

$$\langle\gamma(\phi)\rangle = \int_{\phi_N=0}^{\phi_N=\phi} \gamma(\phi_N)\, dG(N(\phi_N)) + [1 - G(N(\phi))]\gamma(\phi) \quad \textit{film pressure} \Rightarrow$$

$$\langle\sigma_\gamma(\phi)\rangle = \frac{2\langle\gamma(\phi)\rangle}{3r_S} \quad \textit{pressure on solid phase surface} \qquad (25)$$

$$r_S = \frac{V_{SOL}}{S_{TOT}} = \frac{1-c}{c}\frac{V_{TOT}}{S_{BET}} = \frac{1-c}{c} D\theta_o \quad \textit{hydr. rad. of solid phase}$$

$$\langle\sigma_M(\phi)\rangle = \frac{RTDd_L}{M}\int_{\phi_N=0}^{\phi_N=\phi} \sigma_M(\phi,\phi_N)\, dH(N(\phi_N)) \quad \textit{micro pore pressure}$$

$$= \frac{RTDd_L}{M}\left[\log(\phi)H(N_\phi) - \int_{\phi_N=0}^{\phi=\phi_N} \log(\phi_N)\frac{dH(N(\phi_N))}{d\phi_N} d\phi_N\right] \qquad (26)$$

$$\langle\sigma_C\rangle = \frac{U_C(\phi)}{U_{TOT}}\sigma_C(\phi) \quad \textit{capillary pore tension} \qquad (27)$$

7.1.1 Reference system: Granular versus un-broken

The above calculated stresses act on the total system - including voids produced by crushing. They can be transformed as follows to average stresses applying to the original material. It is hereby assumed that condensation stresses are negligible in voids produced by crushing.

$$\frac{\langle\sigma_M\rangle_o}{\langle\sigma_M\rangle} = \frac{\langle\sigma_C\rangle_o}{\langle\sigma_C\rangle} = \frac{1 - c_o}{1 - c} \quad ; \quad \langle\sigma_\gamma\rangle_o = \langle\sigma_\gamma\rangle \tag{28}$$

Volume stresses are considered by Equation 28 to be distributed proportionate to solid phase volume of granular system (1 - c) and original system ($1 - c_o$) respectively. Pore surface added by granulation is considered to be negligible, meaning that surface stresses transform un-changed between granular system and un-broken system.

Remark: As in Section 1.3 subscript "o" is used only temporarily to distinguish one porosity from the other. In subsequent sections we do not use this subscript as the meaning of porosity is evident from the context.

7.2 Analysis

The shrinkage analysis presented in Equation 29, based on results developed in (22), is straight forward. Strains ε are linear quantities. K_S and K are bulk stiffness of solid phase and porous material respectively. The simple result of strain caused by adsorbed moisture is due to the fact previously indicated that the equivalent surface pressure ($\langle\sigma_\gamma\rangle$) acts on the total solid phase surface producing a hydrostatic stress state which implies strain in composite and solid phase to be equal.

$$\varepsilon_M = \frac{\langle\sigma_M\rangle}{3}\left[\frac{1}{K} - \frac{1}{K_S}\right] \qquad \textit{micro pores}$$

$$\varepsilon_C = \frac{\langle\sigma_C\rangle}{3}\left[\frac{1}{K} - \frac{1}{K_S}\right] \qquad \textit{capillary pores} \tag{29}$$

$$\varepsilon_\gamma = \frac{\langle\sigma_\gamma\rangle}{3K_S} \qquad \textit{pore surface}$$

$$\varepsilon_{SH} = \varepsilon_M - \varepsilon_C + \varepsilon_\gamma \qquad \textit{total}$$

The bulk stiffness K of the porous material can be related to bulk stiffness K_S of the solid phase and pore geometry by the following expression developed by the author in (24,21) for isotropic and plane isotropic porous materials, (see also Appendix B)

$$\frac{K}{K_S} \approx \frac{\mu(1-c)}{c+\mu} \quad \textit{with shape factors}$$
$$\mu \approx \begin{cases} 1 & \textit{spherical pores mainly} \\ 2/3 & \textit{cylindrical pores mainly} \\ < 1/3 & \textit{flat pores mainly} \end{cases} \tag{30}$$

The shape factor μ varies with porosity if pore shape varies with porosity. Each pore geometry has its specific shape factor.

Now, shrinkage can be calculated as shown in Equation 31 combining Equations 29 and 30. Bulk moduli can (if not known) be estimated from Young's moduli as indicated in Equation 31. The influence of moisture on stiffness in general (any bulk moduli) can be considered by a moisture factor ß as explained in Equation 32.

$$\varepsilon_M = \frac{\langle\sigma_M\rangle}{3K}\frac{c(1+\mu)}{c+\mu} \;;\; \varepsilon_C = \frac{\langle\sigma_C\rangle}{3K}\frac{c(1+\mu)}{c+\mu}$$
$$\varepsilon_\gamma = \frac{\langle\sigma_\gamma\rangle}{3K}\frac{\mu(1-c)}{c+\mu} \Rightarrow \varepsilon_{SH} = \varepsilon_M - \varepsilon_C + \varepsilon_\gamma \;;\; (K \approx 0.6E) \tag{31}$$

$$\frac{\textit{stiffness}(u)}{\textit{stiffness}(0)} \approx 1 - \beta\frac{u}{u_{FOG}} \tag{32}$$

7.3 Examples

The shrinkage analysis just explained has been applied to the pulp and cellular concrete materials previously considered in this paper subjected to water desorption. The results of the analysis are presented in the following figures. Stiffness quantities (E) are estimated from (25). Moisture factors (ß) on stiffness are estimated from (11, Chap. 11) using the model presented in Equation 32.

MATERIAL	PULP	CELL-CONCR
Figures	Section 7.3.1	Section 7.3.2
E [MPa], μ, ß	500 (⊥), 0.7, 0.7	2000, 1, 0.2

TABLE 3. Material parameters. Any Poisson's ratio is given a value of 0.2. Same materials as in Tables 1 and 2.

7.3.1 Pulp

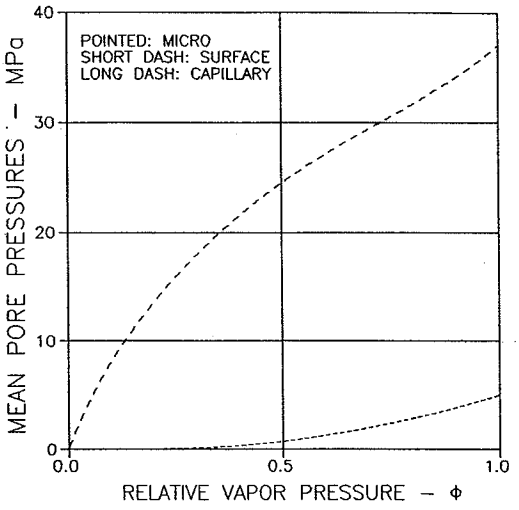

Figure 31. Pulp: Mean pore pressures.

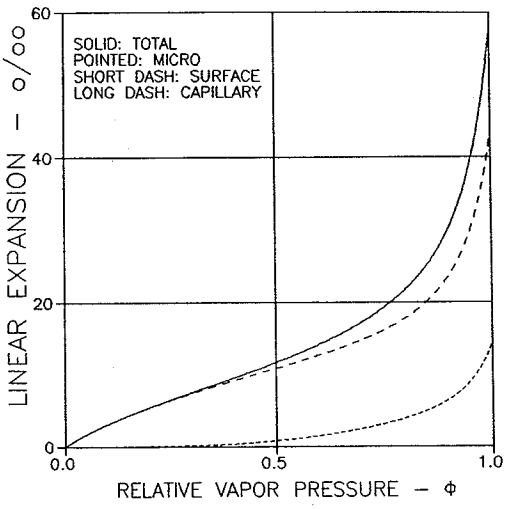

Figure 32. Pulp: Shrinkage perpendicular to fibre direction.

7.3.2 Cellular concrete

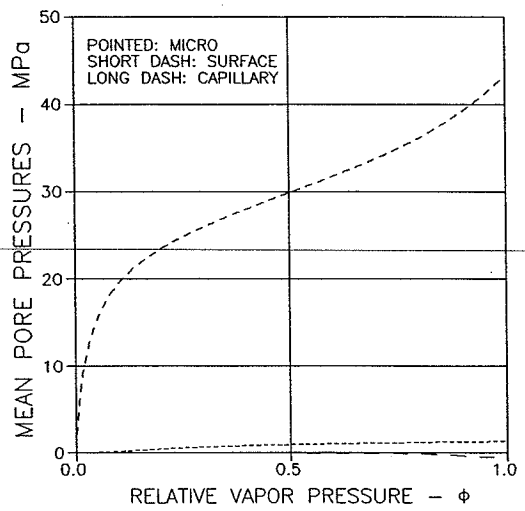

Figure 33. Cell-concrete: Mean pore pressures.

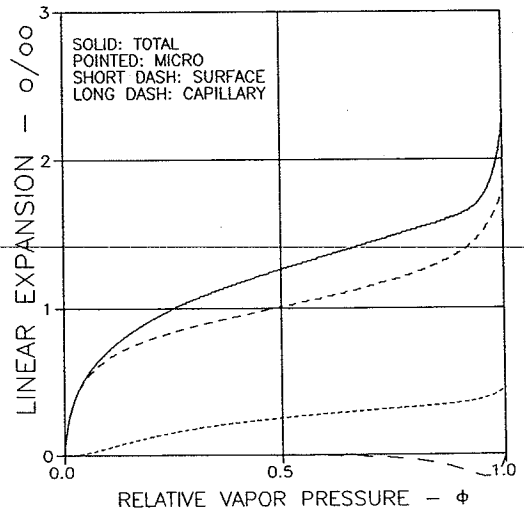

Figure 34. Cell-concrete: Shrinkage.

8. RELIABILITY OF ANALYSIS

An analysis made in Appendix B reveals the following stress and strain results for a porous material exposed to pore pressure. The symbols used are explained in Figure 35.

$$\frac{\varepsilon_P}{\langle\varepsilon\rangle} \approx \frac{\sigma_S}{\langle\varepsilon\rangle E_S} \approx \frac{1 + c}{2c} \quad ; \quad \frac{\langle\sigma_S\rangle}{\langle\varepsilon\rangle E_S} \approx \frac{2}{3} \tag{33}$$

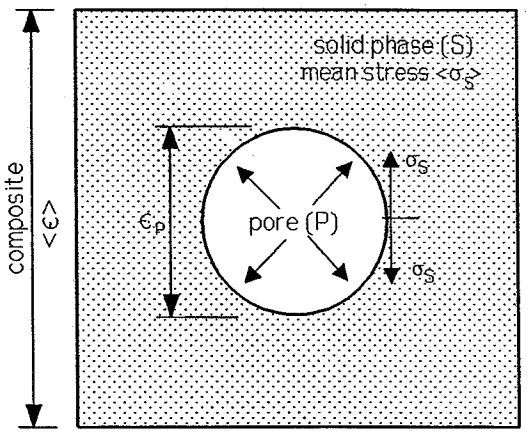

Figure 35. Stress, σ_S is tangential solid stress at void edge. Average solid stress is $\langle\sigma_S\rangle$. Strain from top to bottom of void is ε_P. Average strain of porous material is $\langle\varepsilon\rangle$.

Equation 33 can be used to evaluate the reliability of the pore size analysis and shrinkage analysis suggested in Sections 6 and 7:

- Mean strain $\langle\varepsilon\rangle$ is shrinkage strain ε_{SH}
- Pore strain ε_P is strain of hydraulic radius θ which should not exceed $1/N_C$ where N_C is greatest micro pore radius at vapor pressure considered. If $\varepsilon_P > 1/N_C$ another layer can squeeze in such that actual pore radius becomes one molecule diameter greater than predicted. This will desturb the very important basis of analysis. (If $N_C = N_{MAX}$ then $N_C = N_{MAX} - 1$).

Thus, the most reliable analysis is obtained in vapour pressure areas where the following condition applies.

$$N_C \varepsilon_{SH} \leq \frac{2c}{1 + c} \tag{34}$$

At higher vapour presures, experimental sorption data do not reveal true pore structure information for immediate application in the analysis presented in this paper. Modifications have to be introduced which neutralize the tendency of the experimental technique used to alter the object studied.

Remark: It is implicitly understood that the solid phase can withstand the following stress predicted by Equation 33, and that the associated strain is within acceptable limits of applying the small deformations theory of elasticity.

$$\sigma_S \approx \frac{1 + c}{2c} E_S \varepsilon_{SH} \tag{35}$$

8.1 Examples

8.1.1 Pulp

Porosity is c = 0.5. Shrinkage is $\varepsilon_{SH} \approx 5.5$ % at $\phi = 1$. Greatest micro pore radius is $N_C = N_{MAX} = 14$ at this vapor pressure. Calculational $N_C = N_{MAX} - 1 = 13$. $N_C * \varepsilon_{SH} \approx 0.71$ which just (almost) satifies the condition ≤ 0.67 in Equation 34.

This means that the pore size analysis and shrinkage analysis made can just be considered reliable. Stress $\sigma_S \approx 140$ MPa is predicted by Equation 35 with $E_S \approx 1700$ MPa. This stress is a mean of maximum stress at pores. Higher stresses may develope locally as indicated by Figure 6.

8.1.2 Cellular concrete

Porosity is c = 0.8. Shrinkage is $\varepsilon_{SH} \approx 0.25$ % at $\phi = 1$. Greatest micro pore radius is $N_C \approx 2$ at this vapor pressure. $N_C * \varepsilon_{SH} \approx 0.05$ which satifies the condition ≤ 0.89 in Equation 34.

This means that the pore size analysis and shrinkage analysis made can be considered reliable. Stress $\sigma_S \approx 50$ MPa is predicted by Equation 35 with $E_S \approx 18000$ MPa. As in the previous example local stresses may be found which are higher than σ_S.

9. FINAL REMARKS

Methods have been presented which predict pore size distributions and shrinkage of porous materials from measured sorption data. The method of pore size analysis is consistent with known physical relationships between volume and stress of adsorbed moisture - and between stress and geometry of moisture condensed by capillary actions. The method of shrinkage prediction is based on these relation ships together with composite theory where external response of a porous material can be related to pore pressures and tensions build up during moisture condensation.

Verifications of the methods are presently somewhat difficult. No one knows about real pore size distributions in porous materials - and there are not many experimental results available which combine moisture sorption with associated shrinkage.

However, the shrinkage results obtained compare positively with orders of magnitudes generally observed in experiments: A shrinkage strain of approximately 0.25 ‰ of cellular concrete ($d = 500$ kg/m^3) for example was observed in (26) when drying from $\phi = 1$ to $\phi = 0.43$. Another publication (25) gives the following orders of magnitudes for shrinkage of cellular concrete: 0.2-0.6 ‰ when drying from wet to $\phi = 50$ ‰ - and 1-2 ‰ when drying from wet to completely dry. The same reference (25) tells that shrinkage of wood materials (perpendicular to grain) have the orders of magnitudes: 25-45 ‰ when drying from wet to $\phi = 50$ % - and 40-80 ‰ when drying from wet to completely dry.

As pore size distributions are the basic geometrical in-put in the shrinkage analysis it might then be concluded that the pore size analysis suggested in the paper may also be reasonably accurate.

Limits of the applicability of the methods presented have been considered in Section 8. It seems that materials should not be much softer than pulp perpendicular to fiber direction before modifications of the methods have to be introduced. Building materials which are stiffer (which are the major part) can be analysed directly by the methods presented.

Finally some topics are listed which are of high priority in future research on pore geometry in porous materials and its influence on the mechanical and physical properties of such materials:

- More simultaneous sorp-shrink test should be made as in (27) and (28). Mutual justifications, verifications, and modifications of various analytical methods can be obtained in this way to examine the pore geometry of porous

materials and its influence on the mechanical and physical behavior of such materials.

- More information on T-graphs for various materials is needed. Reliability of predicted pore size distributions is directly proportionate to reliability of T-graphs.
- More information is needed on the proper value of the contact angle between solid and moisture in a porous structure.
- More experiments should consider sorption at vapour pressures less than 10 %. Data in this area are extremely important to improve BET properties. With respect to pore size analysis it is very important that any sorption tests are made until complete equilibrium.
- Efforts should be made to combine pore size analysis based on sorption data (as the one presented in this paper) with methods covering pore radii in fill-up areas.
- More tests should be made to compare sorption data from tests on granulated material with data from tests on un-broken material. Such tests are important in the research on consistent pore size predictions (as in this paper) which require simultaneous predictions with respect to size and surface.
- Pores may have crack shapes which might cause materials destruction during moisture intrusion. Special tests should be made to examine this phenomenon.

10. LIST OF NOTATIONS

Symbols frequently used in the analysis are summarized and briefly explained in the following list. The terms "radius" and "vapour pressure" are used in the meaning "hydraulic radius" and "relative vapour pressure" respectively unless otherwise indicated.

Liquid (water in parenthesis)

R	gas constant, 8.314 J/(Mol*K°)
M	molecule weight (0.01802 kg/Mol)
Γ	surface energy (0.0728 N/m, T = 293 K°)
d_L	density (1000 kg/m^3, T = 293 K°)
D	molecule diameter ($0.30*10^{-9}$ m at T = 293 K°)

Solid and porous material

c	porosity of porous material
d_S	density of solid (kg/m^3)
$d = (1 - c)d_S$	density of porous material (kg/m^3)
$V_{TOT} = c/d$	pore volume (m^3/kg solid)
$V_{SOL} = (1 - c)V_{TOT}/c$	solid phase volume (m^3/kg solid)
E_S	solid phase Young's modulus
ν_S	solid phase Poisson's ratio
E	porous materials Young's modulus
$K_S = E_S/3/(1 - 2\nu_S)$	solid phase bulk modulus
K	porous materials bulk modulus
$\underline{K}_S = E_S/2/(1 - \nu_S)$	solid phase plane stress bulk modulus
$\underline{K}$	porous materials plane stress bulk modulus
μ	shape factor (function) of pore system
ß	stiffness moisture reduction factor

Pore system

r	(hydraulic) pore radius (see subsequent list on sorption)
r_{MAX}	max (hydraulic) pore radius
$\theta = r/D$	normalized radius (with respect to molecule diameter)
θ_{MAX}	normalized max pore radius
A	aspect ratio of typical pore (length/width)
$S_{TOT} = S_{BET}$	total pore surface (see subsequent list on sorption)
$S = S(\theta)$	Surface of pores with radii $\leq \theta$
$V = V(\theta)$	Volume of pores with radii $\leq \theta$
$G = G(\theta) = S/S_{TOT}$	accumulated pore surface distribution
$H = H(\theta) = V/V_{TOT}$	accumulated pore volume distribution
$g = g(\theta) = dG/d\theta$	density function of pore surface distribution
$h = h(\theta) = dH/d\theta$	density function of pore volume distribution

Sorption

ϕ	relative vapour pressure
ϕ_{FOG}	relative vapour pressure at $\phi = 1^-$

α	contact angle between pore wall and capillary meniscus
u	moisture content in porous material (kg/kg solid)
Q,P,M	fit parameters for sorption descriptions
C	heat property factor in BET-parameter
u_{UNI}	weight of uni-molecular layer on solid surface (kg/kg solid) in BET-parameter
u_{ADS}	weight adsorbed on solid surface (kg/kg solid)
$N = u_{ADS}/u_{UNI}$	number of molecule layers adsorbed on free solid surface
$u_{TOT} = V_{TOT}*d_L$	$= cd_L/(d_S(1 - c))$, total moisture content (kg/kg solid)
u_{FOG}	max. moisture content held by adsorption and capillary forces at $\phi = 1^-$ (fog) (kg/kg solid)
$u_{FILL} = u_{TOT} - u_{FOG}$	"fill up" moisture at $\phi = 1$ (kg/kg solid).
u_M	moisture in pores (micro pores) completely filled with adsorbed moisture (kg/kg solid)
u_S	moisture adsorbed on pore surface not associated with micro pores (kg/kg solid)
u_C	moisture in pores bound by capillary forces (kg/kg solid)
$U_I = u_I/u_{UNI}$	normalized moisture content of porous material (I is type of moisture content previously defined)
$S_{TOT} = S_{BET}$	$= u_{UNI}/(D*d_L)$, Total surface of pores (m^2/kg solid)
r_C	(hydraulic) capillary pore radius (m)
$\theta_C = r_C/D$	normalized capillary radius
$r = N*D + r_C$	pore radius (definition) (m)
$\theta = N + \theta_C$	normalized pore radius
$r_o = V_{TOT}/S_{TOT}$	Mean pore radius (m)
$\theta_o = r_o/D = u_{TOT}/u_{UNI}$	normalized mean pore radius
ϕ_{CR}	($\approx$ 0.995) critical vapour pressure beyond which no further capillary moisture is added (gravity forces dominate)

Stress and strain

σ	stress, pressure or tension
ε	linear strain
ε_P	strain of pore radius
σ_S	stress in solid close to pore
$\langle\rangle$	mean quantity
γ	film pressure in adsorbed moisture (N/m)
σ_M	hydraulic pressure in micro pores
σ_γ	normal stress on solid surface due to film pressure
σ_C	hydraulic tension caused by capillary action
ε_M	linear strain of porous material due to micro pore pressure
ε_γ	linear strain of porous material due to film pressure
ε_C	linear strain of porous material du to capillary tension

ε_{SH} total linear shrinkage/swelling strain of material

Granular system

e granular porosity

c_o temporary porosity of un-broken porous material

$c = 1 - (1 - e)(1 - c_o)$ total porosity of granular test system

LITERATURE

1. Brunauer, S., Emmett, P.H. and Teller, E.: "Adsorption of Gases in Multimolecular Layers". J. Am. Ceram. Soc. 60(1938), 309-319.

2. "Stiffness and other physical properties of composites as related to phase geometry and connectivity - Part II: Quantification of geometry", 3rd Symposium on Building Physics in the Nordic Countries, Copenhagen, Sept. 13.-15. 1993. Proceedings Vol. 2 (Bjarne Saxhof, editor) Thermal Insulation Laboratory, Technical University Denmark, 1993, pp 735 - 743.

3. Powers, T.C. and T.L. Brownyard: "Studies of the physical properties of hardened Portland cement paste, Part 3", Journ. Am. Concr. Inst., Proc. vol. 43(1946), 469-504.

4. Nielsen, L. Fuglsang: "Moisture Sorption in Porous Materials - a Rational Fit Procedure". In "Baustoffe - Forschung, Anwendung, Bewährung" (Festschrift für Professor Rupert Springenschmid). Baustoffinstitut, Technische Univerzität München, 1989.

5. Nielsen, L. Fuglsang: "Moisture in porous materials - A modified BET-description", 3rd Symposium on Building Physics in the Nordic Countries, Copenhagen, Sept. 13.-15., 1993. Proceedings Vol. 2 (Bjarne Saxhof, editor) Thermal Insulation Laboratory, Technical University Denmark, 1993, pp 719 - 724.

6. Ahlgren, L.: "Fugtfixering i poröse bygnadsmaterial" (in swedish, Moisture fixation in porous building materials). Thesis, Division of Building Technology, Tech. Uni. Lund, Sweden, 1972.

7. Radjy, F.: "Surface pressure. Capillary condensation. Pore size analysis". and "Swelling and shrinkage", Chapters 19 and 20 respectively in "Kompendium i Bygningsmateriallære: Teoretisk del", ("Text book in building materials, Theoretical part"). Building Materials Lab., Tech. Univ. Denmark, 1971.

8. Gibbs, J.W.: "Collected Works". New Haven, Conn., Yale University Press, 1957.

9. Deryagin, B.V.: "A theory of capillary condensation on the pores of sorbents and of other capillary phenomena taking into account the disjoining action of polymolecular liquid films". Acta Physicho-chimica USSR, 12(1945), 181-200.

10. Powers, T.C., and Brownyard, T.L.: "Studies of the physical properties of hardened Portland cement paste: Part 4". Proc. Am. Concr. Inst. 43(1947), 549 - 602.

11. Illston, J.M., Dinwoodie, J.M., and Smith, A.A.: "Concrete, Timber, and Metals". Van Nostrand Reinhold Co. Ltd., New York 1979.

12. Powers, T.C.: "Mechanisms of shrinkage and reversible creep of hardened cement paste". Int. Conf. on "The structure of concrete and its behavior under

load" London Sept. 1965, Proc. Cement and Concrete Association, London 1968, 319-344.

13. Nielsen, L. Fuglsang: "Sorption, pore size distribution, and shrinkage of porous materials". Build. Mat. Lab., Tech. Univ. Denmark, Tech. report 245, 1991.

14. Jybæk, S.H.: "Water sorption in wood based materials". Build. Mat. Lab., Tech. Uni. Denmark, M.Sc. thesis, 1993.

15. Hansen, K.K.: "Sorption Isotherms". Building Materials Laboratory, Tech. Univ. Denmark, Tech. Rep. 162, 1986.

16. Lykow, A.W.: "Transporterscheinungen in kapillarporösen Körper". Akademie Verlag, Berlin, 1958.

17. Luikov, A.V.: "Heat and mass transfer in capillary-porous bodies". Pergamon Press, Oxford, 1966.

18. Radjy, F. and Sellevold, E.J.: "A Phenomenological Theory for the t-Method of Pore Structure Analysis, Part I: Slit-Shaped Pores". Journ. of Colloid and Interface Science, 39(1972), 367-378.

19. Sellevold, E.J. and Radjy, F.: "A Phenomenological Theory for the t-Method of Pore Structure Analysis, Part II: Circular Cylindrical Pores". Journ. of Colloid and Interface Science, 39(1972), 379-388.

20. Bangham, D.H. and Fakhoury, M.: "The swelling of charcoal. Part I: Preliminary experiments with water vapour, carbon dioxide, ammonia and sulphur dioxide". Proc. Royal Soc., A130(1930), 81-89.

21. Nielsen, L. Fuglsang: "Elasticity and Damping of Porous Materials and Impregnated Materials". Journ. Am. Ceramic. Soc., 67(1984), 93 - 98.

22. Nielsen, L. Fuglsang: "Mechanics of composite material subjected to eigenstress - With special reference to frost resistance of porous brittle material", Danish Building Research Institute, SBI-Bulletin 96(1993).

23. Flood, E.A.: "Adsorption potentials, adsorbent self-potentials and thermodynamic equilibria". In "Solid surfaces and the gas-solid interface", American Chemical Soc., Washington, Advances in Chemistry Series No 33(1961), 249.

24. Nielsen, L. Fuglsang: "Elastic Properties of Two-Phase Materials", Materials Science and Engineering, 52(1982), 39.

25. Nielsen, A.: "Bygningsmaterialers egenskaber", (in danish, Properties of building materials). Build. Mat. Lab., Tech. Uni. Denmark, Tech. report 274, 1992.

26. Nielsen, A.: "Creep of autoclaved aerated concrete" (in swedish). Thesis, Division of Building Technology, Tech. Univ. Lund, Sweden, Bulletin 4(1968).

27. Zheng, Yu: "Pore structure and shrinkage of hardened cement paste, bricks, and sand stone". M.Sc. thesis, Build. Mat. Lab., Tech. Uni. Denmark, 1994.

28. Nielsen, A.: "Sorption and shrinkage of cellular concrete". Progress report 22.03.1994, Building Research Institute, Hørsholm, Denmark, 1994.

29. Kollmann, F.F.P. and W.A. Côté,Jr.: "Principles of wood science and technology, Vol. I: Solid wood", Springer Verlag, Berlin, 1968.

30. Flood, E.A. (ed). 1967. "The solid gas interface". Marcel Dekkers, New York. (Data by S. Brunauer et al. page 737).

31. Timoschenko, S. and J.N. Goodier: "Theory of elasticity", Int. Student Edition, McGraw-Hill Book Comp., New York, 1951.

32. Sokolnikoff, I.S.: "Mathematical theory of elasticity". McGrawHill Book Comp., New York, 1956.

APPENDIX SECTIONS

Appendix A - Miscellaneous

A1. Hypothesis on BET factor C for composites

The following hypothesis is suggested as a model for the BET-factor C of a composite material. The point of departure is Equation 3 in the main text of the paper. Specific composites considered are wood based materials:

$$C = \exp\left[\frac{\Delta}{RT}\right] \quad with\ \Delta = W_A - W_L$$
$$\log C_{COMP} = c_{CELL}\frac{\Delta_{CELL}}{RT} + c_{HEMI}\frac{\Delta_{HEMI}}{RT} + c_{LIGN}\frac{\Delta_{LIGN}}{RT} \qquad \text{(A1)}$$

When calibrated with weight fractions from (11,p119)

Weigth fractions in wood:

$c_{CELL} \approx 0.40 - 0.50\ (0.45)$
$c_{HEMI} \approx 0.20 - 0.25\ (0.25)$
$c_{LIGN} \approx 0.25 - 0.30\ (0.25)$
$c_{EXTR} \approx 0.00 - 0.10\ (0.05)$ (A2)

and contributions to total sorption from (29,p191)

Contributions to total sorption in wood:

CELL: 0.47 (0.45)
HEMI: 0.37 (0.40)
LIGN: 0.16 (0.15) (A3)

we get the result

$$C_{COMP} = \exp\left[\frac{4550c_{CELL} + 6450c_{HEMI} + 2320c_{LIGN}}{RT}\right] \qquad \text{(A4)}$$

A2. Alternative T-graph

Other T-graph formulations may be presented through Equation 6 of the main text. Examples are shown in Figures A1 and A2 using the h_T function presented in Equation A5. The sorption data shown are from free surface tests on calcium silicate hydrates (30) with energy factor C ≈ 130. As N_{MAX} increases Equation A5 becomes Equation 7.

$$h_T(\phi) = \frac{1 - \phi^q}{1 - \phi} + \frac{\phi^{qp}}{1 - \phi^p}(1 - \phi^{pm}) \qquad with$$

$$q = N_{MAX} - \frac{15}{N_{MAX}} \; ; \; m = \frac{15}{N_{MAX}} \; ; \; p = 1 + \frac{20}{N_{MAX}} \tag{A5}$$

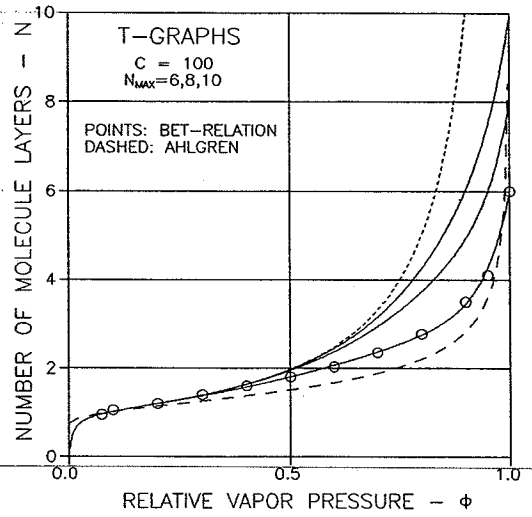

Figure A1. T-graphs for N_{MAX} = 6, 8, and 10 with C = 100. Experimental data from (30). Dashed graph is Ahlgren's expression as modified in Equation 8.

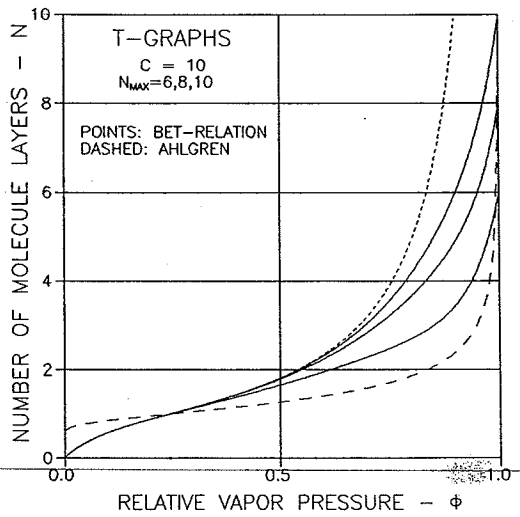

Figure A2. T-graphs for N_{MAX} = 6, 8, and 10 with C = 10. Dashed graph predicted by Equation 8.

A3. Pore size distributions in fill-up area

Pore size distributions cannot be found by the method presented in the paper when radii are greater than $\approx 10^{-7}$ m (fill-up area). The analyse may proceed with estimated distributions of pore surface, of pore volume, or moisture content with respect to radii. A log-linear pore surface distribution has been used in Section 6.2.2. Two other easy distribution assumptions are subsequently suggested by which associated distributions can be determined analytically by Equation 21. Subscript MIN and MAX mean value at $\phi = 1^-$ and at completely filled material respectively. U_{FILL} is moisture content between these extreme states.

Log-linear moisture distribution

$$U = U_{MIN} + U_{FILL}\frac{\log(\theta/\theta_{MIN})}{\log(\theta_{MAX}/\theta_{MIN})} \Rightarrow$$
$$G = G_{MIN} + \frac{U_{FILL}}{N_{MAX}\log(\theta_{MAX}/\theta_{MIN})}\log\left[\frac{1 - N_{MAX}/\theta}{1 - N_{MAX}/\theta_{MIN}}\right] \quad \text{(A6)}$$

Max pore radius is determined introducing G = 1. We get

$$1 - G_{MIN} = \frac{U_{FILL}}{N_{MAX}\log(\theta_{MAX}/\theta_{MIN})}\log\left[\frac{1 - N_{MAX}/\theta_{MAX}}{1 - N_{MAX}/\theta_{MIN}}\right] \quad \text{(A7)}$$

Log-linear pore volume distribution

$$H = H_{MIN} + (1 - H_{MIN})\frac{\log(\theta/\theta_{MIN})}{\log(\theta_{MAX}/\theta_{MIN})} \Rightarrow$$
$$U = U_{MIN} + \frac{\theta_o(1 - H_{MIN})}{\log(\theta_{MAX}/\theta_{MIN})}\left[N_{MAX}\left[\frac{1}{\theta} - \frac{1}{\theta_{MIN}}\right] + \log\left[\frac{\theta}{\theta_{MIN}}\right]\right] \quad \text{(A8)}$$

Max pore radius is determined introducing G = 1. We get

$$\frac{1}{\theta_{MAX}} = \frac{1}{\theta_{MIN}} + \frac{1}{N_{MAX}}\left[\frac{U_{FILL}}{\theta_o(1 - H_{MIN})} - 1\right]\log\left[\frac{\theta_{MAX}}{\theta_{MIN}}\right] \quad \text{(A9)}$$

Appendix B - Stress-strain of porous material

Adsorbed moisture creates a state of pressure in a porous material which produces expansion of the material. Does this expansion give space for more molecules than assumed in the pore size analysis presented in this paper. If it does, then predicted pore size distributions become false and counteracting modifications have to be introduced into the prediction method.

This problem is the subject of this appendix. Solutions are developed for pore strain in porous materials subjected to pore pressure. Spin-off results are stiffness of porous materials and solid stresses throughout the material. The analysis is based on a hollow cylinders model and a hollow spheres model of a porous material. The analysis is made rather short and self explaining. The results are used and commented in Section 8 of the main text.

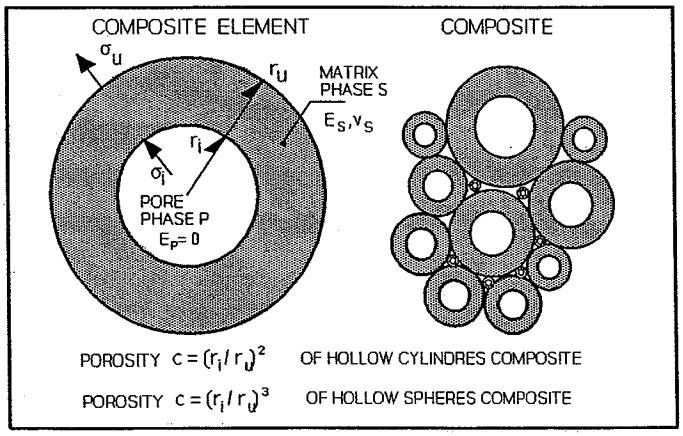

Figure B1. Models of porous material.

B1. Models

The models used are illustrated in Figure B1: Pores are hollow cylindres or they are hollow spheres in composite elements such that void ratio in each element equals the porosity of the total porous material. For volumetric actions every composite element act with no interaction to other elements, meaning that each composite element can be analysed independently with results which also apply to the total composite material.

Tube subjected to compressive load

For the present purpose the following tube solutions have been developed from Timoschenko and Goodier (31, pp 59 and 66).

$$\sigma_r = \frac{\sigma_O + c\sigma_I - (\sigma_O + \sigma_I)(r_I/r)^2}{1 - c} \quad ; \quad c = \left[\frac{r_I}{r_O}\right]^2$$

$$\sigma_\theta = \frac{\sigma_O + c\sigma_I + (\sigma_O + \sigma_I)(r_I/r)^2}{1 - c} \qquad \text{(B1)}$$

$$u_O = \frac{r_O}{E(1 - c)}\left[c(1 + \nu)(\sigma_I + \sigma_O) + (1 - \nu)(c\sigma_I + \sigma_O)\right]$$

$$u_I = \frac{r_I}{E(1 - c)}\left[(1 + \nu)(\sigma_I + \sigma_O) + (1 - \nu)(c\sigma_I + \sigma_O)\right]$$

Sphere subjected to compressive load

For the present purpose the following spherical solutions have been developed from Sokolnikoff (32, pp 344 and 345).

$$\sigma_r = \frac{\sigma_O + c\sigma_I - (\sigma_O + \sigma_I)(r_I/r)^3}{1 - c} \quad ; \quad c = \left[\frac{r_I}{r_O}\right]^3$$

$$\sigma_\theta = \frac{\sigma_O + c\sigma_I + \tfrac{1}{2}(\sigma_O + \sigma_I)(r_I/r)^3}{1 - c} \qquad \text{(B2)}$$

$$u_O = \frac{r_O}{E(1 - c)}\left[\tfrac{1}{2}c(1 + \nu)(\sigma_O + \sigma_I) + (1 - 2\nu)(c\sigma_I + \sigma_O)\right]$$

$$u_I = \frac{r_I}{E(1 - c)}\left[\tfrac{1}{2}(1 + \nu)(\sigma_I + \sigma_O) + (1 - 2\nu)(c\sigma_I + \sigma_O)\right]$$

B2. Hollow cylinders composite

Plane hydrostatic stiffness

The following stiffness expression for materials with tube pores is easily obtained from Equation B1. The result is illustrated in Figure B2

$$2\underline{K} = \frac{\sigma_O}{u_O/r_O} = E_S \frac{1 - c}{1 + c - \nu_S(1 - c)} \quad (\textit{from Eq. B1 with } \sigma_I = 0)$$
$$\underline{K} = \underline{K}_S \frac{(1 - \nu_S)(1 - c)}{1 + c - \nu_S(1 - c)} \quad ; \quad \left[\frac{\underline{K}}{\underline{K}_S} = \frac{1 - c}{1 + c/0.67} \quad at\ \nu_S = 0.2 \right] \qquad \text{(B3)}$$

Stress and strain due to pore pressure

The following expressions for strains and stresses in materials with parallel tube pores are also easily obtained from Equation B1. Subscripts P and S have the meanings explained in Figure 35 of the main text. Average quantity is denoted by <>.

Average strain and pore strain

$$\langle \varepsilon \rangle = \frac{\sigma_I}{2\underline{K}} - \frac{\sigma_I}{2\underline{K}_S} = \frac{\sigma_I}{E_S} \frac{2c}{1 - c}$$
$$\varepsilon_P = \frac{u_I}{r_I} = \frac{\sigma_I}{E_S} \frac{1 + c + \nu_S(1 - c)}{1 - c} \quad ; \quad (\textit{from Eq. B1: } \sigma_O = 0) \qquad \text{(B4)}$$

Average solid stress and solid stress at pore

$$\frac{\langle \sigma_S \rangle}{\sigma_I} = \frac{c}{1 - c} \quad (\textit{simple equlibrium condition})$$
$$\frac{\sigma_S}{\sigma_I} = \frac{\sigma_\theta(r=r_I)}{\sigma_I} = \frac{1 + c}{1 - c} \quad ; \quad (\textit{from Eq. B1 with } \sigma_O = 0) \qquad \text{(B5)}$$

Strains and stresses versus mean strain

Of special interest are the following expressions derived from Equations B4 and B5. They relate strains and stresses as illustrated in Figure B3 to the average strain of the porous material considered

$$\frac{\varepsilon_P}{\langle\varepsilon\rangle} = \frac{1 + c + \nu_S(1 - c)}{2c}$$
$$\frac{\sigma_S}{\langle\varepsilon\rangle} = \frac{E_S(1 + c)}{2c} \quad ; \quad \frac{\langle\sigma_S\rangle}{\langle\varepsilon\rangle} = \frac{E_S}{2} \tag{B6}$$

B3. Hollow spheres composite

Hydrostatic stiffness

The following stiffness expression for materials with spherical pores is easily obtained from Equation B2. The result is illustrated in Figure B2

$$3K = \frac{\sigma_O}{u_O/r_O} = \frac{2E_S(1-c)}{(1+\nu_S)c + 2(1-2\nu_S)} \quad (\sigma_I = 0 \text{ in Eq. B2}) \Rightarrow$$

$$K = K_S \frac{2(1-2\nu_S)(1-c)}{2(1-2\nu_S) + c(1+\nu_S)} \quad ; \quad \left[\frac{K}{K_S} = \frac{1-c}{1+c} \text{ at } \nu_S = 0.2\right] \tag{B7}$$

Stress and strain due to pore pressure

The following expressions for strains and stresses in materials with spherical pores are also easily obtained by Equation B2. Subscripts P and S have the meanings explained in Figure 35 of the main text. Average quantity is denoted by <>.

Average strain and pore strain

$$\langle\varepsilon\rangle = \frac{\sigma_I}{3K} - \frac{\sigma_I}{3K_S} = \frac{3}{2}\frac{\sigma_I}{E_S}\frac{(1-\nu_S)c}{1-c}$$

$$\varepsilon_P = \frac{u_I}{r_I} = \frac{\sigma_I}{E_S}\frac{1+\nu_S+2c(1-2\nu_S)}{2(1-c)} \quad ; \quad (\sigma_O = 0 \text{ in Eq. B2}) \tag{B8}$$

Average solid stress and solid stress at pore

$$\frac{\langle\sigma_S\rangle}{\sigma_I} = \frac{c}{1-c} \quad (\textit{simple equlibrium condition})$$

$$\frac{\sigma_S}{\sigma_I} = \frac{\sigma_\theta(r=r_I)}{\sigma_I} = \frac{1+2c}{2(1-c)} \quad ; \quad (\sigma_O = 0 \text{ in Eq. B2}) \tag{B9}$$

Strains and stresses versus mean strain

Of special interest are the following expressions derived from Equations B8 and B9. They relate strains and stresses as illustrated in Figure B4 to the average strain of the porous material considered

$$\frac{\varepsilon_P}{\langle\varepsilon\rangle} = \frac{1 + \nu_S + 2c(1 - 2\nu_S)}{3(1 - \nu)c}$$
$$\frac{\sigma_S}{\langle\varepsilon\rangle} = \frac{E_S(1 + 2c)}{3c(1 - \nu_S)} \quad ; \quad \frac{\langle\sigma_S\rangle}{\langle\varepsilon\rangle} = \frac{2}{3}\frac{E_S}{1 - \nu} \tag{B10}$$

B4. Conclusions

Stiffness of porous material

Stiffness of a hollow cylinders composite and of a hollow spheres composite are shown in Figure B2 as derived from Equations B3 and B7 respectively with ν_s = 0.2. The results presented can also be obtained from the authors more general theory on composite materials composite (24,21,22) from which Equation B11 is reproduced with constant shape factors μ.

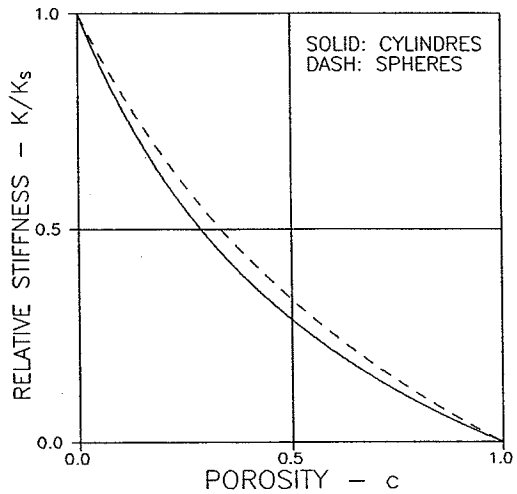

Figure B2. Stiffness of hollow cylindres composite and hollow spheres composite when ν_s = 0.2.

Equation B11 applies strictly only for isotropic and plane-isotropic porous materials where the shape factor $0 \leq \mu \leq 1$. It can, however, be used as a good approximation also when other materials are considered. Even for stiffness along the parallel pores in orthotropic pore system. In this case $\mu = \infty$ is introduced.

$$\frac{COMP\text{-}STIFFNESS}{SOLID\text{-}STIFFNESS} \approx \frac{1 - c}{1 + c/\mu} = \frac{\mu(1 - c)}{\mu + c} \qquad \text{(B11)}$$

$$\mu \approx \begin{cases} 1 & \textit{spherical pores mainly} \\ 2/3 & \textit{cylindrical pores mainly} \\ < 1/3 & \textit{flat pores mainly} \end{cases} ; \ (\textit{Shape factors})$$

Remark: In the original version of Equation B11 (24,21,22) $\mu = \mu(c)$ is a shape function. For the present purpose, however, we may consider μ as a constant when geometry defined in Equation B11 is the one applying at the specific porosity considered.

Stress and strain due to pore pressure

Stress and strain at pores in a hollow cylinders composite and of a hollow spheres composite are presented in Figures B3 and B4 as derived from Equations B6 and

B10 respectively with $\nu_S = 0.2$. An approximate summary for both composites is given in Equation B12.

$$\frac{\varepsilon_P}{\langle\varepsilon\rangle} \approx \frac{\sigma_S}{\langle\varepsilon\rangle E_S} \approx \frac{1+c}{2c} \quad ; \quad \frac{\langle\sigma_S\rangle}{\langle\varepsilon\rangle E_S} \approx \frac{2}{3} \tag{B12}$$

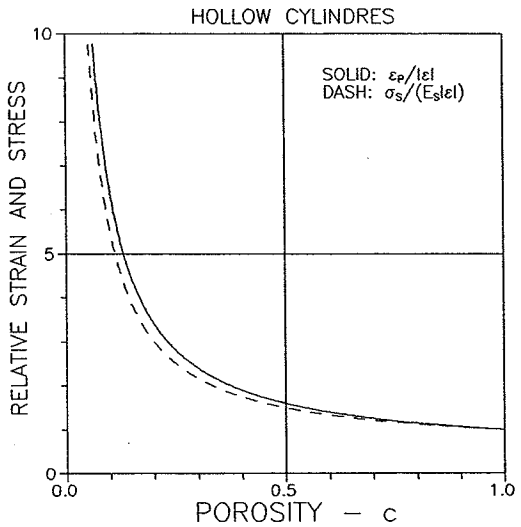

Figure B3. Pore strain and solid stress at pore edge in a hollow cylindres composite. $\nu_S = 0.2$

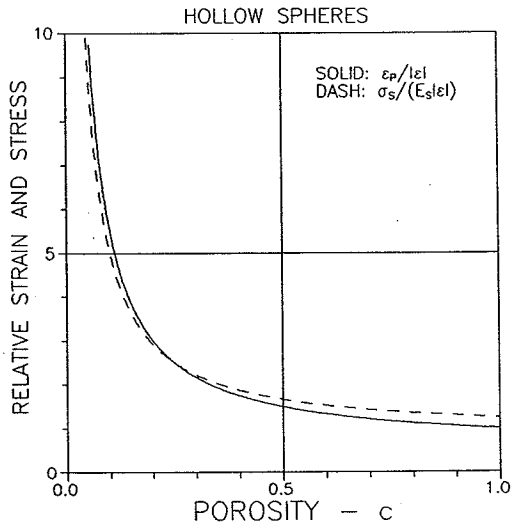

Figure B4. Pore strain and solid stress at pore edge in hollow spheres composite. $\nu_S = 0.2$.